UNIVERSITÀ
DI PAVIA

Expression, purification, and characterization of human Cyclin-Dependent Kinase-Like 1 (CDKL1)

Espressione, purificazione e caratterizzazione della proteina umana CDKL1 (Cyclin-Dependent Kinase-Like 1)

Supervisor:

Professor Federico Forneris

Co-supervisors:

Dr. Emmanuele Crespan

Experimental thesis by

Lorena Isabel Ruiz Fontalvo

Academic Year 2025/2026

Riassunto

Le protein chinasi sono regolatori fondamentali della progressione del ciclo cellulare e di altri processi cellulari essenziali, rappresentando una delle classi più importanti di bersagli terapeutici nella medicina moderna. Infatti, molti farmaci antitumorali attualmente utilizzati in clinica agiscono attraverso la modulazione dell'attività chinasica. Nonostante la loro rilevanza biologica e farmacologica, molti membri del chinoma umano rimangono ancora poco caratterizzati. Tra questi, la famiglia delle chinasi *cyclin-dependent kinase-like* (CDKL) rappresenta uno dei gruppi di chinasi meno studiati, sebbene evidenze crescenti abbiano implicato diversi membri della famiglia CDKL in patologie umane, incluse malattie del neurosviluppo e cancro.

CDKL1 rimane particolarmente poco studiata sia a livello biochimico sia funzionale. I suoi substrati e i suoi meccanismi regolatori sono ancora sconosciuti. D'altro canto, le evidenze disponibili suggeriscono che CDKL1 sia coinvolta nella regolazione della progressione del ciclo cellulare, della proliferazione e dell'apoptosi. Inoltre, il suo ruolo nel cancro sembra essere complesso e dipendente dal contesto tissutale, indicando che CDKL1 potrebbe rappresentare un bersaglio terapeutico rilevante ma ancora poco definito. Questa tesi si è posta l'obiettivo di stabilire un sistema sperimentale per la caratterizzazione biochimica di CDKL1 e di esplorarne la suscettibilità all'inibizione.

A questo scopo, CDKL1 è stata espressa in E. Coli e purificata mediante diverse tecniche cromatografiche, ottenendo una resa e grado di purezza adeguati alla valutazione della sua attività enzimatica. Il saggio di attività chinasica è stato ottimizzato in modo sistematico, valutando parametri sperimentali chiave quali la selezione del substrato, il tempo di reazione, il pH, la composizione del tampone e la concentrazione di ATP. È stato identificato un substrato peptidico compatibile con l'attività di CDKL1 e sono stati determinati parametri cinetici utili a descrivere la reazione chinasica in vitro. Inoltre, è stato condotto uno screening di inibitori utilizzando sia inibitori chinasici ad ampio spettro sia un piccolo pannello di ellagitannini.

Staurosporina, acido chebulagico e vescalagina sono stati identificati come efficaci inibitori dell'attività di CDKL1 nelle condizioni sperimentali impiegate. Nel complesso, questo lavoro costituisce la prima descrizione dell'attività chinasica in vitro di CDKL1. Il saggio sviluppato rappresenta un utile punto di partenza per studi futuri volti a definire la specificità di substrato, i meccanismi regolatori e la modulazione farmacologica di CDKL1, e potrebbe supportare lo sviluppo di nuovi inibitori più potenti e selettivi per indagare il ruolo biologico di questa chinasi.

UNIVERSITÀ
DI PAVIA

Dipartimento di Biologia e Biotecnologie
"Lazzaro Spallanzani"

Laurea Magistralis in Molecular Biology and Genetics

Expression, purification, and characterization of human Cyclin-Dependent Kinase-Like 1 (CDKL1)

Supervisor:
Professor Federico Forneris

Co-supervisors:
Dr. Emmanuele Crespan

Experimental thesis by
Lorena Isabel Ruiz Fontalvo

Academic Year 2024/2025

Acknowledgements

I would like to express my deepest gratitude to all the people who supported me throughout this journey.

First, I would like to thank my supervisor, Crespo, and my thesis director, Professor Forneris, for their guidance, patience, and support during the development of this work. They truly made the effort not only to help me, but also to understand me. Their advice, knowledge, and encouragement have been invaluable, not only for this thesis, but also for my growth as a student, as a researcher, and as a person. For this, I am infinitely grateful.

I am also sincerely grateful to my lab companions, Elisa M. and Elisa — or, as we used to say, *Elisa grande* and *Elisa bimba* — as well as Noemi and Elena, for their help, kindness, and for sharing both the challenges and the lighter moments of everyday life in the lab. Their presence made this experience far more meaningful and enjoyable.

To my friends — Simone, who stayed by my side through some of my darkest moments; Anja, always ready to listen to every complaint and somehow also prepared with medication just in case; Mattia, who was always there, even when none of us knew what to do; and Mel, who would share every party with me and still wake up early for the lab the next day — thank you. Your support, encouragement, and understanding carried me through the difficult times and helped me celebrate the good ones. This achievement would not have felt the same without you by my side.

I would also like to thank the ESN group, with a special mention to Marcello, Elena, and Babi, for making me feel welcome, seen, and embraced, even when the language barrier felt very real. More broadly, I am grateful to everyone in the association for all the nights we shared, all the projects we worked on, and all the joy and laughter along the way.

Finally, I would like to thank my family. Without their love, encouragement, and support, I would not even be here. To my mother, who gave me life, the ability to dream, and the freedom to search for my own path. To my father, for his constant love and his wise words. And to my sister, for giving me purpose and the will to keep going in life.

To everyone who, in one way or another, walked beside me and helped me reach this point, thank you. This work is also a reflection of your support.

Abstract

Protein kinases are key regulators of cell-cycle progression and other essential cellular processes, making them one of the most important classes of therapeutic targets in modern medicine. Indeed, many anticancer agents currently in clinical use act through modulation of kinase activity. Despite their biological and pharmacological relevance, many members of the human kinome remain poorly characterized. Among these, the cyclin-dependent kinase-like (CDKL) family represents one of the least understood kinase groups, although increasing evidence has implicated different CDKL members in human disease, including neurodevelopmental disorders and cancer.

CDKL1 remains particularly understudied at both biochemical and functional levels. Its substrates and upstream regulatory mechanisms are still unknown, yet available evidence suggests that CDKL1 participates in the regulation of cell-cycle progression, proliferation, and apoptosis. In addition, its role in cancer appears to be complex and tissue-dependent, indicating that CDKL1 may represent a relevant but poorly defined therapeutic target. The present work therefore aimed to establish an experimental framework for the biochemical characterization of CDKL1 and to explore its susceptibility to inhibition by selected compounds.

To achieve this, CDKL1 was produced and purified using a large-scale strategy that yielded recombinant protein of suitable purity for downstream analyses. Kinase activity assays were then systematically optimized by evaluating key experimental parameters, including substrate selection, reaction time, pH, buffer composition, and ATP concentration. A peptide substrate compatible with CDKL1 activity was identified, and kinetic parameters were determined to define appropriate assay conditions. In addition, inhibitor screening was performed using both broad-spectrum kinase inhibitors and a small panel of ellagitannins.

Staurosporine, chebulagic acid, and vescalagin were identified as effective inhibitors of CDKL1 activity under the assay conditions employed. Overall, this work provides, to our knowledge, the first in vitro biochemical platform for the systematic analysis of CDKL1 kinase activity and inhibition. The assay developed here represents a useful starting point for future studies aimed at defining CDKL1 substrate specificity, regulatory mechanisms, and pharmacological modulation, and may support the development of more potent and selective compounds to investigate the biological role of this kinase.

Table of contents

1. Introduction

1.1. Protein-kinases

The human body functions through highly coordinated cells, each fulfilling a specific role within complex biological systems. Such coordination is essential not only in humans but across all living organisms, where precise regulation ensures proper development, adaptation, and survival(1). This level of organization depends on numerous intracellular processes that must themselves be tightly controlled in both space and time. To achieve this, cells employ a wide range of regulatory proteins that modulate the activity of other proteins, among which protein kinases play a central and indispensable role(2).

Protein kinases constitute a large and diverse family of enzymes that catalyze the transfer of a phosphate group (PO_4^{3-}) from adenosine triphosphate (ATP) to specific amino acid residues within protein substrates, in a process known as phosphorylation (3). This post-translational modification represents a fundamental mechanism for regulating protein activity, stability, localization, and interactions. Through reversible phosphorylation events, protein kinases function as key modulators of signaling pathways, enabling cells to respond dynamically to internal and external stimuli(4). Consequently, protein kinases regulate essential cellular processes, including cell growth, metabolism, differentiation, and apoptosis (programmed cell death), and are therefore critical for maintaining cellular homeostasis and proper physiological function(2).

The human genome encodes more than 500 protein kinases, collectively referred to as the Human Kinome(2). It has been estimated that as many as 30% of human proteins undergo phosphorylation at some stage, including protein kinases themselves(5). This extensive level of phosphorylation enables the formation of complex signaling cascades, in which sequential kinase activation can amplify and propagate signals, ultimately leading to diverse cellular responses(2)(3). Through these mechanisms, protein kinases regulate a wide range of cellular pathways, particularly those involved in signal transduction(2,6).

Protein kinases can be classified according to the amino acid residues they phosphorylate. Based on this criterion, they are grouped into three main categories(3):

- **Tyrosine (Tyr or Y)-specific kinases**: These enzymes phosphorylate tyrosine residues and are primarily involved in signal transduction processes, often associated with growth factor receptors and membrane-associated signaling pathways(4,7).
- **Serine/Threonine (Ser/Thr or S/T) kinases**: These kinases phosphorylate the hydroxyl (–OH) groups of serine and threonine residues. Most human kinases belong to this group and are regulated through multiple mechanisms. Consequently, they play key roles in processes such as cell differentiation, proliferation, apoptosis, and embryonic development(3,7).
- **Dual-specificity kinases**: These enzymes can phosphorylate serine, threonine, and tyrosine residues, allowing them to function at critical points within signaling cascades(3,4).

In addition to classification based on substrate specificity, protein kinases are further grouped into seven major families according to sequence homology and structural features(3):

- **AGC family**: This group comprises serine/threonine kinases related to cAMP-dependent protein kinase (PKA), cGMP-dependent protein kinase (PKG), and protein kinase C (PKC). These kinases participate in the regulation of metabolism, cell growth, and survival(3,8).
- **CaMK family**: Calcium/calmodulin-dependent protein kinases are activated by increases in intracellular Ca^{2+} levels. They phosphorylate a variety of substrates, including transcription factors, and are therefore important regulators of gene expression. Members include CaMK I–V (3).
- **CK1 family**: Originally identified as casein kinase 1, this family consists of serine/threonine kinases involved in multiple signaling pathways. CK1 isoforms regulate processes such as Wnt signaling, circadian rhythms, DNA repair, transcription, and nucleocytoplasmic transport of transcription factors(3).
- **STE family**: Named after yeast sterile kinases, this group includes several kinase subfamilies that function in mitogen-activated protein kinase (MAPK) cascades. These kinases act sequentially, with upstream members activating downstream kinases, ultimately leading to MAPK activation(3).

- **TK family**: Tyrosine kinases specifically phosphorylate tyrosine residues and are often associated with receptor tyrosine kinases (RTKs) located at the cell surface, where they mediate extracellular signal detection and transmission(3,9).
- **TKL family**: Tyrosine kinase-like kinases share sequence similarity with tyrosine kinases but function as serine/threonine kinases. Members include RAF, MLK, LRRK, IRAK, and RIPK, and they participate in diverse signaling pathways(3).
- **CMGC family**: This group includes cyclin-dependent kinases (CDKs), mitogen-activated protein kinases (MAPKs), glycogen synthase kinase 3 (GSK3), and CDC-like kinases (CLKs). These kinases regulate essential cellular processes such as cell cycle progression, signal transduction, embryonic development, and RNA processing(10,11).

Together, these classification systems highlight both the diversity and the functional importance of protein kinases in cellular regulation, providing a framework for understanding their roles in physiological and pathological contexts.

In addition to protein kinases, protein phosphatases play a complementary role in the regulation of phosphorylation-dependent signaling. These enzymes catalyze the removal of phosphate groups from phosphorylated proteins by hydrolyzing phosphoric acid monoesters, restoring the hydroxyl group on the target residue, and returning the protein to its non-phosphorylated state(3). This reversible process of phosphorylation and dephosphorylation constitutes a dynamic regulatory cycle that is essential for the precise control of protein function and cellular signaling pathways. The coordinated activity of kinases and phosphatases enables tight temporal and spatial regulation of signaling networks, ensuring appropriate cellular responses to internal and external stimuli(12,13)

Given their central role in cellular regulation, protein kinases are involved in a wide range of biological processes. Consequently, dysregulation of kinase activity is associated with numerous pathological conditions, most notably cancer, where aberrant phosphorylation can promote uncontrolled cell proliferation and survival(4,14). As a result, protein kinases have emerged as one of the most important classes of therapeutic targets in modern medicine(15). A growing number of small-molecule kinase inhibitors have been developed, several of which are currently in clinical use or under clinical investigation (Table 1).

Table 1. Some small-molecule inhibitors of protein kinases undergoing human clinical trials.(15)

Kinase targeted	Inhibitor	Company	Disease	Status
Tyrosine kinases				
ABL (KITR, PRGFR)	Gleevec (Glivec, STI-571)	Novartis	Cancer	FDA approval, May 2001
EFGR	ZD1839 (Iressa)	AstraZeneca	Cancer	Phase III
	OSI774	OSI Pharmaceuticals/Roche Genentech	Cancer	Phase III
EFGR, ERB2R	CI1033	Pfizer	Cancer	Phase I
	EKB569	Wyeth-Ayerst	Cancer	Phase I
	GW2016	GlaxoSmithKline	Cancer	Phase I
	PKI166	Novartis	Cancer	Phase I
VEGFR (PDGFR, FGFR)	SU6668	Pharmacia Corporation	Cancer	Phase I
VEGFR	PTK787/ZK222584	Novartis/Schering-Plough	Cancer	Phase II
VEGFR (EGFR)	ZD6474	AstraZeneca	Cancer	Phase I
NGFR	CEP2583	Cephalon	Cancer	Phase II
Serine/Threonine kinases				
PKC, KITR, PDGFR?	PKC412	Novartis	Cancer, retinopathy	Phase I
CDKs?	Flavopiridol	Aventis	Cancer	Phase II
CDK2	CYC202	Cyclacel	Cancer	Phase I
MKK1	PD184352	Pfizer	Cancer	Phase I
RAF?	BAY43-906	Onyx Pharmaceuticals/Bayer	Cancer	Phase I
CHK1, PKC, others?	UCN-01	Kyowa Hakko	Cancer	Phase I
mTOR	CCI779	Wyeth-Ayerst	Cancer	Phase II
	RAD001	Novartis	Cancer	Phase I
	Rapamycin (Sirolimus)	Wyeth-Ayerst	Immunosuppression	FDA approval, 1999
ROCK?	HA1077 (AT877, fasudil)	Asahi Chemical Industry	Cerebral vasospasm	Approved in 1995 (Japan)
PKCβ	LY333531	Eli Lilly	Diabetic retinopathy	Phase III
P38/SAPK2a	SB281832	GlaxoSmithKline	Rheumatoid arthritis	Phase I
	BIRB0796	Boehringer Ingelheim	Rheumatoid arthritis	Phase II
	Ro320-1195	Roche	Rheumatoid arthritis	Phase I
MLK	CEP-1347	Cephalon	Neurodegeneration	Phase I

1.2. CDK-Like kinases

CDK-Like kinases (CDKL) are part of the CMGC superfamily. This group comprises more than 60 serine/threonine kinases organized into several families, including DYRKs, GSKs, CLKs, SRPKs, RCKs, MAPKs, and CDKs, from which CDKL kinases derive their name(16). Members of the CMGC group share a conserved catalytic architecture, characterized by an N-terminal and a C-terminal lobe flanking an ATP-binding cleft, a structural organization typical of eukaryotic protein kinases(16)(17). In addition, they possess a characteristic CMGC insert within the C-lobe, which functions as a structural element facilitating regulatory protein–protein interactions (Fig. 1). This conserved structural framework underlies both the functional similarities and the specialized regulatory mechanisms observed within this kinase family(16).

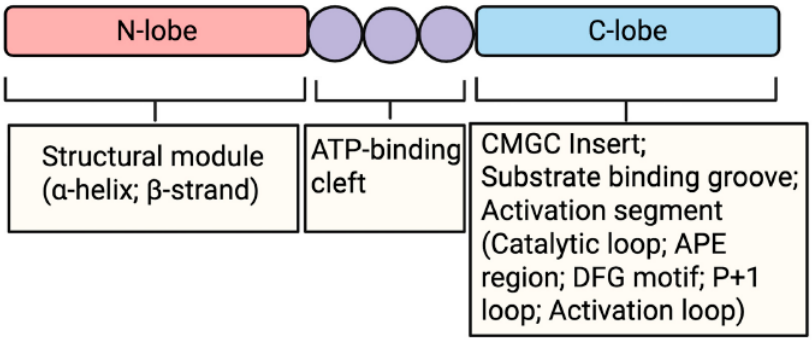

Figure 1. Conserved structure of CMGC kinases. (16)

It is worth noting that, although CMGC kinases are often described within discrete signaling cascades, their structural similarities and overlapping substrate specificities place them within a highly interconnected regulatory network. Rather than functioning in isolation, these kinases continuously influence one another's activity, collectively integrating mitogenic, metabolic, and stress-related signals. Through this coordinated network, CMGC kinases contribute to the fine-tuned regulation of cellular responses and ultimately play a decisive role in determining cell fate(16,18).

Cyclin-dependent kinases (CDKs) conform to the conserved structural architecture characteristic of the CMGC group(16). Their N-terminal lobe is predominantly composed of β-sheets, while the C-terminal lobe is enriched in α-helices, with the catalytic active site located in the cleft between the two domains(19). CDKs typically range from approximately 250 to 1500 amino acids in length and are distinguished by their dependence on regulatory protein subunits known as cyclins. These proteins provide essential structural elements required for kinase activation, and their interaction with the catalytic domain is necessary for CDK functionality. Cyclins therefore act as key regulatory units, modulating both the activity and substrate specificity of CDKs(16,19).

Based on their mode of regulation, CDKs can be broadly classified into two functional groups. The first group comprises CDKs that are associated with multiple cyclins and are primarily involved in controlling cell cycle progression. The second group includes CDKs that interact with a single cyclin partner and are mainly implicated in the regulation of transcription. This distinction reflects the diverse roles of CDKs within the cell, linking cell cycle control with gene expression and broader regulatory processes(19).

The CDKL represents one of the least characterized groups within the CMGC kinase superfamily. These kinases derive their name from their structural similarity to CDKs, as they share key features such as conserved ATP-binding domains, a serine/threonine kinase active site, and a putative cyclin-binding region(16,18). However, unlike CDKs, CDKL kinases do not appear to require cyclins for their activation, suggesting different structural regulatory mechanisms. The CDKL family comprises five human serine/threonine kinases, designated CDKL1–5, which remain relatively underexplored(18).

Canning et al. solved the structures of most members of the CDKL family in 2018. CDKL kinases exhibit a conserved N-terminal region that contains the catalytic domain, including the ATP-binding site and the putative cyclin-binding interface. This suggests that small-molecule inhibitors targeting the ATP-binding pocket may be effective across multiple members(20). In contrast, the C-terminal region is more variable, contributing to potential functional divergence. Another distinctive feature of CDKL kinases is the presence of a TXY phosphorylation motif within the activation loop, like that observed in MAPKs, which may facilitate substrate recognition, particularly for proteins containing DEF (Asp-Glu-Phe) motifs(20).

Although CDKL family members share high sequence homology and structural similarity, they differ in their genomic localization and expression patterns across tissues(16). CDKL1 is expressed in multiple tissues, including the brain, lungs, and kidneys, whereas CDKL2 and CDKL3 are predominantly expressed in the testis and brain. CDKL5 shows strong expression in the brain, while CDKL4 is expressed at relatively low levels in human tissues. At the subcellular level, CDKL1, CDKL2, and CDKL5 have been reported to localize to both the nucleus and the cytoplasm in various cell types. Despite these observations, there is currently no clear consensus regarding the precise cellular and molecular functions of CDKL kinases(18).

As members of the CMGC family, CDKL kinases are expected to participate in phosphorylation-dependent signaling; however, their specific substrates and regulatory pathways remain poorly characterized(16). Despite sharing common structural features, growing evidence suggests that individual CDKL members may fulfil distinct biological roles, reflecting differences in their expression patterns, subcellular localizations, and regulatory mechanisms. Given the limited and fragmented knowledge currently available, a comprehensive understanding of the CDKL family requires the examination of each member individually(16).

1.2.1 Members of the CDKL family

CDKL5 is the most extensively studied member of the CDKL family. It is highly expressed in the brain, suggesting a prominent role in neuronal development and function. Dysfunction of CDKL5 was initially associated with Rett syndrome; however, it has since been recognized as a distinct condition, termed CDKL5 deficiency disorder (CDD), characterized by early-onset epileptic encephalopathy and severe neurodevelopmental impairment(21). This distinction highlights the critical importance of CDKL5 in neural processes. In line with this, recent studies have implicated CDKL5 in the regulation of primary cilia, which acts as key signaling hubs during neuronal development, suggesting that CDKL5 may contribute to neurodevelopmental processes through the modulation of cilia-dependent signaling(21,22).

Despite the increasing interest in CDKL5, relatively limited information is available regarding its specific substrates. Several candidate substrates have been identified in vitro, including DNMT1, MeCP2, NGL-1, Amph1, HDAC4, MAP1S, EB2, and SMAD3. The identification of CDKL5 substrates has proven challenging due to the incomplete understanding of its substrate recognition mechanisms. Although some studies have suggested a preference for the RPXS motif, this does not fully explain substrate specificity, as proteins such as glutamate receptor 5 and septin 4, which contain this motif, are not phosphorylated by CDKL5. This suggests that additional structural determinants are required for substrate recognition(21).

Structurally, CDKL5 contains a conserved N-terminal catalytic domain and a more variable C-terminal region(20), the activation loop of CDKL5 contains the conserved sequence ANYTEYVAT (Fig. 2), which is predicted to require phosphorylation for full kinase activation(21). Evidence suggests that CDKL5 may undergo autophosphorylation in vitro, particularly upon stimulation with brain-derived neurotrophic factor (BDNF), although the specific residues involved remain unclear. In terms of deactivation, CDKL5 has been shown to be dephosphorylated by protein phosphatase 1 (PP1) following NMDA receptor stimulation, a process that appears to promote its cytoplasmic localization(21).

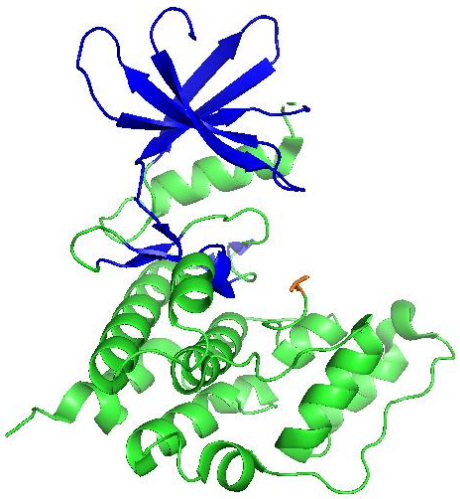

Figure 2. CDKL5 structure.
In blue conserved N-lobe, C-terminal in green, in orange TEY motif.

CDKL5 is known to shuttle between the nucleus and the cytoplasm, and its subcellular localization may be dynamically regulated depending on cellular context (7). Consistent with its role in cilia-dependent signaling, disruption of CDKL5 has been associated with defects in ciliary function, which may contribute to the neurological phenotype observed in CDKL5 deficiency disorder(18,22). Additionally, there is evidence that DYRK1A can phosphorylate CDKL5, although the functional consequences of this interaction remain to be fully elucidated(18).

Among the members of the CDKL family, **CDKL4** represents the least characterized kinase. Current knowledge is largely limited to sequence annotation and expression data, with few studies addressing its biochemical activity or physiological function. Available evidence suggests that CDKL4 is localized in the cytoplasm; however, its precise cellular role remains undefined(18). Studies investigating the involvement of CDKL4 in cancer are also limited. Lin et al. reported that an increased copy number of CDKL4 is associated with a higher risk of recurrence and mortality in colorectal cancer. Additionally, elevated CDKL4 mRNA expression has been observed in osteosarcoma tissues(23). Despite these observations, the functional significance of CDKL4 in tumorigenesis remains unclear. Overall, CDKL4 remains poorly characterized compared to other members of the CDKL family, with limited functional and molecular data available.

CDKL3 is a relatively better-characterized member of the CDKL family, although its molecular functions remain incompletely understood. Structurally, it contains a conserved N-terminal region and a variable C-lobe with an αJ helix, the activation loop contains a TDY motif (Fig. 3)(20). It is predominantly expressed in the testis and brain and, in contrast to CDKL5, appears to be primarily localized in the cytoplasm. Functional studies have suggested that CDKL3 plays a role in cell cycle regulation, as its disruption has been shown to impair progression from the G0/G1 phase to the S phase and to induce G2-phase arrest *in vitro*. In addition, depletion of CDKL3 has been associated with decreased phosphorylation of Akt, although current evidence is insufficient to establish Akt as a direct substrate of the kinase. These findings indicate a potential involvement of CDKL3 in key signaling pathways regulating cell proliferation and survival(18).

A growing body of evidence supports a role for CDKL3 in tumorigenesis. Silencing of CDKL3 has been shown to induce apoptosis in multiple cancer cell types, including glioma, triple-negative breast cancer, and prostate cancer cells, although the underlying mechanisms appear to differ depending on the cellular context(18). In triple-negative breast cancer, CDKL3 has been reported to inhibit the p53 signaling pathway and to stabilize STAT1, thereby suppressing apoptosis, the precise molecular mechanisms remain to be fully elucidated. Furthermore, CDKL3 has been implicated in the regulation of autophagy, with studies demonstrating that it may function as an inhibitor of autophagy through activation of the Akt–mTORC1 pathway, a well-established negative regulator of autophagy(18).

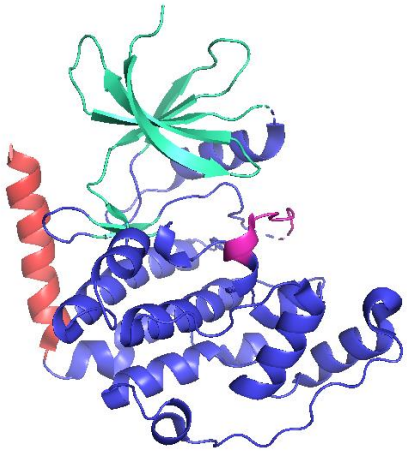

Figure 3. CDKL3 structure.
In green conserved N-lobe, in blue C-lobe, in pink TDY activation motif, αJ helix in red.

Consistent with these functional observations, aberrant expression of CDKL3 has been reported in several malignancies, including anaplastic large cell lymphoma, esophageal squamous cell carcinoma, cholangiocarcinoma, prostate cancer, and colorectal carcinoma. In general, increased CDKL3 expression is associated with enhanced proliferation, migration, and invasive capacity, whereas its knockdown results in reduced tumor cell growth, impaired cell cycle progression, and increased apoptosis(18). Mechanistically, CDKL3 has been shown to promote glioma progression through the regulation of RRM2 and activation of the JNK signaling pathway, while in prostate cancer, it has been proposed to inhibit CBL-mediated ubiquitination of STAT1. In esophageal squamous cell carcinoma, CDKL3 has been linked to ATG5 activation, further supporting its involvement in autophagy-related processes. Notably, pharmacological inhibition of CDKL3 expression, for example by curcumol, has been reported to exert anti-cancer effects in certain tumor models, suggesting potential therapeutic relevance(18).

In addition to its role in cancer, CDKL3 has also been implicated in neuronal development. Gene inactivation has been associated with neurodevelopmental defects, including intellectual disability. Experimental studies have shown that CDKL3 is enriched in neuronal nuclei and is required for proper axon and dendrite morphogenesis, with its depletion leading to reduced dendritic branching, length, and overall complexity. Taken together, these findings indicate that CDKL3 may function as a regulator of both cellular proliferation and neuronal development, although further studies are required to fully elucidate its molecular mechanisms and physiological roles(18).

CDKL2 is a comparatively less investigated member of the CDKL family and displays a tissue-specific expression pattern, being predominantly expressed in the kidney, brain, and lungs. At the subcellular level, CDKL2 has been reported to localize to both the nucleus and the cytoplasm. Functionally, it appears to be responsive to extracellular signals, as it can be stimulated by epidermal growth factor (EGF) without requiring prior phosphorylation. Nevertheless, phosphorylation of the TDY activation motif by upstream kinases such as MEK1 has also been reported, suggesting that CDKL2 activity may be regulated through multiple mechanisms(18).

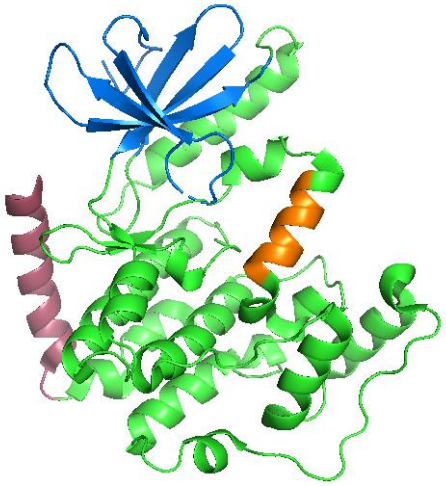

Figure 4. CDKL2 structure.
In blue conserved N-lobe, in green C-lobe, in orange TDY motif and in pink αJ helix.

The role of CDKL2 in cancer is complex and, in some cases, contradictory. On one hand, CDKL2 has been associated with pro-tumorigenic functions. For instance, it has been shown to be more highly expressed in mesenchymal breast cancer cell lines compared to epithelial counterparts, where it promotes epithelial–mesenchymal transition (EMT) through activation of a ZEB1/E-cadherin/β-catenin positive feedback loop. On the other hand, several studies have reported reduced CDKL2 expression in different tumor types, including gliomas, renal clear cell carcinoma, and gastric cancer. In glioma, decreased CDKL2 expression has been correlated with tumor grade, Ki-67 expression, and poorer overall survival, particularly in diffuse gliomas. Similarly, downregulation of CDKL2 in gastric cancer has been associated with advanced disease features, while its overexpression has been shown to inhibit cell proliferation and invasion in vitro(18).

Conversely, other studies have reported increased CDKL2 expression or gene copy number in certain cancers, such as gastric cancer, where it has been associated with HER2-positive status and reduced overall survival. These discrepancies may be attributed to differences in sample size, tumor heterogeneity, or methodological approaches across studies(18). Importantly, despite these conflicting findings, there is a consensus that alterations in CDKL2 expression are not sufficient to serve as an independent prognostic biomarker.

In addition to expression changes, epigenetic regulation of CDKL2 has also been reported. Aberrant DNA methylation of the CDKL2 gene has been observed in several cancers, including hepatocellular carcinoma, HER2-positive breast cancer, and prostate cancer. This methylation is negatively correlated with CDKL2 mRNA expression and is associated with various clinicopathological features, such as patient age, sex, and tumor size. Furthermore, CDKL2 methylation has been incorporated into multi-gene prognostic models, demonstrating its potential utility in predicting patient outcomes in hepatocellular carcinoma(18). Overall, the available evidence suggests that CDKL2 may play context-dependent roles in cancer, acting either as a tumor promoter or suppressor depending on the cellular and molecular environment. However, the lack of consistent mechanistic insights highlights the need for further studies to clarify its biological functions and regulatory pathways.

Taken together, the available evidence indicates that, although members of the CDKL family share a conserved structural framework, they exhibit considerable functional diversity and remain unevenly characterized. CDKL5 has been the most extensively studied, particularly in the context of neurological disorders, whereas CDKL3 and CDKL2 have been increasingly associated with cancer-related processes, including cell cycle regulation, apoptosis, and tumor progression. In contrast, CDKL4 remains largely unexplored, with limited functional data available and only preliminary associations with disease.

This variability in the depth of knowledge across CDKL family members highlights a broader challenge in understanding their biological roles, as many aspects of their substrate specificity, regulatory mechanisms, and physiological functions remain unclear. Within this context, CDKL1 occupies an intermediate position: while it has been implicated in several cellular processes, particularly in cancer biology, it remains significantly less characterized than CDKL5 and lacks comprehensive mechanistic understanding. Existing studies suggest a role in the regulation of cell proliferation and survival; however, its molecular targets and signaling pathways have not been fully elucidated. Given these limitations, CDKL1 represents a particularly relevant subject for further investigation.

1.2.2. CDKL1

Cyclin-dependent kinase-like 1 (CDKL1), also known as KKIALRE or p42, was the first member of the CDKL family to be cloned based on its sequence similarity to CDK1. The CDKL1 gene is located on chromosome 14q21.3 and encodes two isoforms of approximately 276 and 358 amino acids(24). Similarly to other members of the CMGC superfamily, CDKL1 possesses a conserved N-terminal catalytic domain and shares significant sequence homology with cyclin-dependent kinases, including the presence of motifs associated with ATP binding and kinase activity (Fig. 5). In addition, CDKL1 contains the conserved MAPK-like TXY activation motif, suggesting a role in phosphorylation-dependent signaling pathways(20).

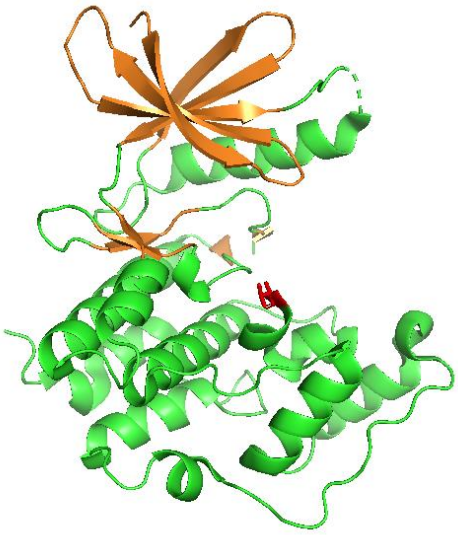

Figure 5. CDKL1 structure. N-lobe in orange, C-lobe in green. In red the TXY motif.

CDKL1 is expressed in several human tissues, including the brain, kidney, and lungs, and has been detected in both the nucleus and the cytoplasm(18). Within the central nervous system, CDKL1 expression has been observed in astrocytes, particularly in white matter, perivascular glial end-feet, and subpial glial structures, indicating a potential role in glial biology(25). Interestingly, CDKL1 and its close homolog CDKL2 exhibit mutually exclusive expression patterns in reproductive tissues, with CDKL1 predominantly expressed in the ovaries and CDKL2 in the testis, suggesting that these kinases may contribute to tissue-specific signaling processes in highly differentiated systems(26).

Although the molecular functions of CDKL1 remain incompletely characterized, several studies provide insight into its potential biochemical activity and regulatory mechanisms. CDKL1 has been shown to phosphorylate histones and synthetic peptides containing consensus motifs such as XSPX, supporting its classification as an active serine/threonine kinase(25,27). Its activity appears to be responsive to extracellular signals, as epidermal growth factor (EGF) has been reported to activate CDKL1 independently of prior phosphorylation, indicating the existence of alternative regulatory mechanisms(26).

Emerging evidence also implies CDKL1 in the regulation of cilia development, although current data are largely derived from non-mammalian models such as *Danio rerio* and *Caenorhabditis elegans*. In these systems, CDKL1 orthologs have been shown to influence ciliary length, acting as negative regulators of cilia elongation(28). Loss or increased levels of CDKL-1 activity result in abnormal ciliary morphology, highlighting the importance of CDKL1 structural integrity for ciliary function. Notably, CDKL1 localizes to distinct ciliary sub compartments compared to CDKL5, suggesting that these kinases may perform non-overlapping roles within cilia-related processes(20). Although the relevance of these findings to human biology remains to be fully established, the high degree of sequence conservation across species supports the possibility that CDKL1 may contribute to cilia-dependent signaling pathways in higher organisms(27).

Consistent with a role in developmental signaling, studies in zebrafish have shown that knockdown of the CDKL1 homolog results in significant morphological abnormalities, including defects in brain and eye development, body axis curvature, and pericardial edema. These phenotypes are accompanied by reduced expression of key developmental regulators such as neurogenin1 and Sonic hedgehog (SHH), indicating a potential involvement of CDKL1 in neurodevelopmental pathways. Furthermore, functional interactions between CDKL1 and SHH signaling have been suggested, as modulation of CDKL1 expression influences SHH activity in the developing floor plate(27).

The emerging evidence linking CDKL1 to the regulation of cell cycle progression, signal transduction, and cilia-associated developmental pathways highlights its potential role as a key modulator of cellular homeostasis. Given that these processes are frequently dysregulated in tumorigenesis, increasing attention has been directed toward the involvement of CDKL1 in cancer. Indeed, a growing body of experimental data demonstrates that aberrant expression of CDKL1 is associated with tumor development and progression across multiple cancer types, supporting its role as a functionally relevant regulator of oncogenic processes.

Although CDKL1 remains less characterized than CDKL5, accumulating evidence consistently links it to the regulation of cell proliferation and tumor progression, making it one of the most promising yet understudied members of the CDKL family.

CDKL1 role in cancer

CDKL1 expression has been reported to be elevated in several malignancies, including colorectal cancer(24), gastric cancer(26), non-small cell lung cancer(28), and breast cancer(29), indicating a broad involvement in tumor biology. In colorectal cancer, CDKL1 overexpression has been linked to tumor progression, while its depletion has been shown to impair cell proliferation and disrupt transcriptional regulation associated with RNA polymerase II and chromosome maintenance(24).

A consistent finding across multiple cancer models is the involvement of CDKL1 in the regulation of the cell cycle. CDKL1 knockdown has been associated with cell cycle arrest, although the specific regulatory mechanisms appear to be context dependent. In melanoma, depletion of CDKL1 results in increased expression of the cyclin-dependent kinase inhibitor p21 and decreased CDK2 levels(30), whereas in colorectal cancer it leads to upregulation of p15 and retinoblastoma protein (Rb), alongside reduced activity of CDK4 and cyclin D1(24). These observations suggest that CDKL1 may modulate cell cycle progression through distinct regulatory pathways depending on the cellular context.

In addition to its role in proliferation, CDKL1 has been implicated in the regulation of apoptosis. Knockdown of CDKL1 promotes apoptotic responses in several types of cancer, including gastric cancer and oral squamous cell carcinoma, where increased expression of pro-apoptotic markers such as Bax and cleaved caspase-3 has been observed(27,28). Conversely, CDKL1 overexpression has been associated with reduced sensitivity to chemotherapeutic agents, suggesting a role in promoting cell survival and therapy resistance(29).

The involvement of CDKL1 in cancer is further supported by studies demonstrating its impact on treatment response. In breast cancer cell lines, silencing of CDKL1 induces G2/M phase arrest and enhances sensitivity to chemotherapeutic agents(29). Similarly, in oral squamous cell carcinoma, high CDKL1 expression reduces sensitivity to hydroxycamptothecin by inhibiting apoptosis through decreased ATM phosphorylation and reduced caspase-3 activation(31). In contrast, in non-small cell lung cancer, CDKL1 overexpression has been associated with increased DNA damage signaling and enhanced sensitivity to radiotherapy, indicating that its role in treatment response may vary depending on the therapeutic context(28).

At the molecular level, CDKL1 has also been shown to interact with key regulatory proteins involved in tumor progression. Notably, CDKL1 can modulate the activity of Y-box binding protein 1 (YBX1), a transcriptional regulator implicated in proliferation, metastasis, and immune evasion. Through this interaction, CDKL1 suppresses the recruitment of YBX1 to the PD-L1 promoter, thereby inhibiting PD-L1 transcription. This mechanism has been associated with enhanced immune sensitization, particularly when CDKL1 overexpression is combined with radiotherapy and anti-PD-L1 treatment, resulting in increased activation of $CD8^+$ T cells(28).

Collectively, these findings demonstrate that CDKL1 plays a multifaceted role in cancer, contributing to the regulation of cell proliferation, apoptosis, DNA damage response, and immune-related signaling pathways. Although the precise molecular mechanisms underlying these effects remain incompletely defined, the consistent association of CDKL1 with tumor progression and treatment response highlights its potential as both a biomarker and a therapeutic target in oncology.

Despite this growing evidence, no selective CDKL1 inhibitors are currently available, and the structural determinants governing ligand recognition remain poorly understood. Consequently, the identification and characterization of novel CDKL1 modulators represents a crucial step towards therapeutical potential evaluation. Among natural components with demonstrated kinase-inhibitory properties, ellagitannins have attracted increasing attention due to their ability to interfere with signaling pathways involved in tumor progression.

1.3. Ellagitannins

Ellagitannins (ETs) are a class of bioactive polyphenols belonging to the group of hydrolysable tannins, including compounds such as corilagin, pedunculagin, punicalagin, castalagin, vescalagin, geraniin, sanguiin derivatives, and chebulagic acid(32). They are widely distributed in fruits and nuts such as pomegranates, berries, and walnuts (Table 2). Structurally, ETs consist of one or more hexahydroxydiphenoyl (HHDP) groups esterified to a glucose core, resulting in a high degree of structural diversity(32,33).

Table 2. Contents of EA in fruits, nuts, beverages (mg/100g of fresh weight), and seeds (mg/g). Total EA estimated after acid hydrolysis to include ETs on the estimation(33).

Food	Ellagic acid	Reference	Food	Ellagic acid	Reference
Fruits			*Fruits*		
Apple	Nd	Kähkönen et al. (2001)	Rose hip	109.6	Koponen et al. (2007)
Apple (red)	Nd	Daniel et al. (1989)	Red currant	Nd	Kähkönen et al. (2001)
Arctic bramble	390	Määttä-Riihinen et al. (2004)	Rowanberry	Nd	Kähkönen et al. (2001)
Bilberry	Nd	Kähkönen et al. (2001)	Sea buckthorn	1.0	Koponen et al. (2007)
Blackberries	150 ± 12.0	Daniel et al. (1989)	Strawberries	63 ± 9.0	Daniel et al. (1989)
Black currant	Nd	Kähkönen et al. (2001)		81–184	Kähkönen et al. (2001)
Black raspberries	90	Wada and Ou (2002)		31	Mattila and Kumpulainen (2002)
Bog-whortleberry	Nd	Kähkönen et al. (2001)		65–85	Määttä-Riihinen et al. (2004)
Boysenberries	70	Wada and Ou (2002)	Strawberry, Honeoye	77.6	Koponen et al. (2007)
Cashews	Nd	Daniel et al. (1989)	Strawberry, Jonsok	79.9	Koponen et al. (2007)
Cherry	Nd	Daniel et al. (1989)		40.3 ± 7.5	Häkkinen et al. (2000)
Chokeberry	Nd	Kähkönen et al. (2001)	Strawberry, Polka	68.3	Koponen et al. (2007)
Cloudberry	315.1	Koponen et al. (2007)	Strawberry jam	24.5	Koponen et al. (2007)
	1090–1423	Kähkönen et al. (2001)		17-29.5	Da Silva Pinto et al. (2007)
	360	Määttä-Riihinen et al. (2004)	Tangelo	Nd	Daniel et al. (1989)
Cowberry	Nd	Kähkönen et al. (2001)	Tangerine	Nd	Daniel et al. (1989)
Cranberry	Nd	Kähkönen et al. (2001)	Yellow raspberry	1900	Määttä-Riihinen et al. (2004)
	12.0 ± 0.4	Daniel et al. (1989)	*Nuts*		
Crowberry	Nd	Kähkönen et al. (2001)	Brazil nuts	Nd	Daniel et al. (1989)
Evergreen blackberries	60	Wada and Ou (2002)	Peanuts	Nd	Daniel et al. (1989)
Gooseberry	Nd	Kähkönen et al. (2001)	Pecans	33 ± 0.3	Daniel et al. (1989)
Kiwi	Nd	Daniel et al. (1989)	Walnuts	59 ± 0.1	Daniel et al. (1989)
Navel oranges	Nd	Daniel et al. (1989)	*Beverages*		
Marionberries	73	Wada and Ou (2002)	Cognac	31–55 mg/L	Clifford and Scalbert (2000)

Peach	Nd	Daniel et al. (1989)	Oak age - red wine	9.4 mg/mL	Glabasnia and Hofmann (2006)
Pear	Nd	Daniel et al. (1989)	Whiskey	1.2 mg/mL	Glabasnia and Hofmann (2006)
Pink grapefruit	Nd	Daniel et al. (1989)	White grape	Nd	Daniel et al. (1989)
Raspberry	263.7	Koponen et al. (2007)	White grapefruit	Nd	Daniel et al. (1989)
	150 ± 10.0	Daniel et al. (1989)	*Seeds*		
	1692–1794	Kähkönen et al. (2001)	Black raspberry	6.7	Bushman et al. (2004)
Raspberry (wild)	270	Määttä-Riihinen et al. (2004)	Red raspberry	8.7	Bushman et al. (2004)
Red raspberry "Ottawa"	70.8 ± 2.8	Kähkönen et al. (2001)	Boysenberry	30	Bushman et al. (2004)
Red raspberry	47	Wada and Ou (2002)	Marion blackberry	32	Bushman et al. (2004)
	103 ± 3.3	Daniel et al. (1989)	Evergreen blackberry	21	Bushman et al. (2004)
	160	Mattila and Kumpulainen (2002)	Longan	1.6	Soong and Barlow (2006)
			Mango	1.2	Soong and Barlow (2006)

Upon hydrolysis, ETs release ellagic acid (EA), which can be further metabolized by the gut microbiota into urolithins. These metabolites are absorbed into systemic circulation and can reach multiple target organs, including the intestine and prostate, indicating that ET-derived compounds may exert systemic biological effects(34). However, this activity is likely influenced by the limited bioavailability of the parent compounds and by tissue exposure to downstream metabolites rather than intact high-molecular-weight(35).

1.3.1. Ellagitannins in cancer models

The anticancer activity of ellagitannins is thought to result from the combined modulation of multiple signaling pathways rather than from a single molecular target. Depending on the cellular context, ellagitannins and their metabolites can interfere with protein kinases, cell-cycle regulators, inflammatory pathways, and oxidative stress responses, ultimately reducing proliferation, inhibiting cell-cycle progression, and producing apoptosis. Ellagitannins and their principal derivative, ellagic acid, exhibit a broad spectrum of biological activities, with consistent evidence supporting antioxidant and anticancer effects(33,35).

Across both experimental and review studies, these compounds have been shown to reduce cell proliferation, promote apoptosis, impair migration and invasion, and suppress angiogenesis in multiple

cancer models(35,36). In colon cancer models, pomegranate-derived ellagitannins and urolithins decreased HT29 cell proliferation in a dose- and time-dependent manner, with cell-cycle arrest preceding cell death(34,35). In leukemia cells, ellagic acid induced caspase-3-dependent apoptosis(35,36), while in glioblastoma xenografts, it suppressed tumor growth alongside reduced expression of Akt, Notch, cyclin D1, CDK2, and CDK6 expression(36,37).

Notably, these biological effects should not be interpreted solely because of direct kinase inhibition by intact ellagitannins. Several studies emphasize that in vivo activity is constrained by factors such as low bioavailability, interindividual variation in gut microbial metabolism to urolithins, and the limited concordance between in vitro potency and achievable systemic concentrations(35). A central and consistent effect of ET-derived compounds is the disruption of cell-cycle progression. In multiple cancer models, treatment with ET-rich extracts or ellagic acid induces cell-cycle arrest at different phases, associated with the downregulation of key kinases and the upregulation of cell-cycle inhibitors (35).

The strongest direct kinase-centered evidence within this chemical class concerns receptor tyrosine kinases involved in angiogenesis. Ellagic acid has been shown to inhibit VEGFR-2 tyrosine kinase activity and to suppress downstream MAPK and PI3K/Akt signaling in endothelial cells, while also reducing endothelial proliferation, migration, tube formation, aortic sprouting, and neo vessel formation in vivo(38). Molecular docking studies further support this mechanism, placing ellagic acid within the ATP-binding region of the VEGFR-2 kinase domain through hydrogen bonding and aromatic interactions, thereby providing a structural basis for direct kinase inhibition (38).

At the molecular level, these phenotypic effects are closely associated with modulation of key oncogenic signaling pathways. Ellagic acid has been shown to inhibit the Wnt/β-catenin pathway in colon cancer and oral oncogenesis models, reducing nuclear β-catenin levels and downstream transcriptional activity(39). Similarly, inhibition of the PI3K/Akt pathway has been reported in lung cancer and anaplastic thyroid cancer models, leading to decreased proliferation, migration, and invasion. Given the central role of these pathways in tumor progression, their modulation represents a critical mechanism underlying the anticancer effects of ETs(39). Additional evidence implicates PKC-, JNK-, p38-, and STAT-associated pathways. A tumor-focused review summarized the inhibition of PKC, VEGFR-2, Notch, and COX-2 signaling among the major mechanisms of ellagic acid activity(35,36).

Within the CMGC kinase family, cyclin-dependent kinases (CDKs) represent key regulators of cell-cycle progression. Ellagic acid has been identified as a potent inhibitor of CDK6, exhibiting a concentration-dependent reduction in kinase activity with an IC_{50} of 3.053 μM(40). Mechanistic studies demonstrate that EA binds to the ATP-binding pocket of CDK6 with high affinity, suggesting direct inhibition of its catalytic activity. In addition, EA reduces CDK6 expression at the translational level in breast cancer cell lines, further contributing to its antiproliferative effects(40).

Among CDKs, CDK6 has the clearest direct evidence as a molecular target. In the same study, ellagic acid treatment resulted in decreased colony formation, induction of apoptosis, and downregulation of CDK6 expression in human breast cancer cell lines (40). Molecular docking and molecular dynamics simulations further indicated that ellagic acid occupies the ATP-binding pocket of CDK6, stabilizes a closed kinase conformation, and maintains key hydrogen bonding interactions over time(40).

Other CDKs appear to be affected more indirectly. In HT29 colon cancer cells treated with pomegranate-derived polyphenols, S-phase arrest was associated with downregulation of CDK A and B1, while ellagic acid and punicalagin modulated cyclin E, cyclin A, and cyclin B1 expression during cell-cycle arrest(34). In glioblastoma xenografts, ellagic acid reduced CDK2 and CDK6 expression alongside inhibition of Akt and Notch signaling(41). Similarly, in pancreatic cancer models, decreased expression of CDK2 and CDK6 has been associated with G1 arrest following ellagic acid exposure(36).

Given the structural and functional similarities between CDKL1 and other members of the CMGC kinase family, including CDKs and MAPKs, it is plausible that ET-derived compounds may also interact with CDKL1. The demonstrated ability of ellagic acid to bind the ATP-binding pocket of CDK6 suggests that similar interactions could occur with structurally related kinases sharing conserved catalytic domains. Furthermore, the capacity of ETs to modulate key signaling pathways, including PI3K/Akt and Wnt/β-catenin, aligns with the known roles of CDKL1 in regulating cell proliferation, apoptosis, and signal transduction in cancer. Since CDKL1 has been implicated in the control of these processes, its inhibition by polyphenolic compounds such as ETs represents a plausible mechanism underlying their observed anticancer effects.

Although direct evidence of CDKL1 inhibition by ellagitannins is currently lacking, the convergence of structural similarity, kinase inhibition potential, and pathway modulation supports the hypothesis that these compounds may act as modulators of CDKL1 activity. This provides a rationale for further investigation into their potential as therapeutic agents targeting CDKL1 in cancer.

2. Research objective

Cyclin-dependent kinase-like 1 (CDKL1) is a poorly characterized serine/threonine protein kinase belonging to the CMGC kinase group and to the CDK-like family. Although CDKL kinases share structural features with cyclin-dependent kinases, including a conserved catalytic domain and an ATP-binding pocket, their regulatory mechanisms, cellular substrates and physiological functions remain incompletely understood. Among the CDKL family members, CDKL1 is still largely underexplored, despite emerging evidence suggesting that it may be involved in relevant cellular processes and may have a role in pathological contexts, including cancer biology.

Protein kinases represent one of the most successful classes of therapeutic targets, particularly in oncology. However, the discovery and validation of new kinase targets require the availability of reliable biochemical tools, including recombinant active protein, robust enzymatic assays and defined assay conditions suitable for inhibitor testing. In the case of poorly characterized kinases such as CDKL1, these preliminary biochemical steps are particularly important, because limited information is available regarding optimal substrates, reaction conditions and sensitivity to small-molecule inhibitors.
The general aim of this thesis was therefore to establish a biochemical platform for the expression, purification and enzymatic characterization of human CDKL1. To this end, recombinant CDKL1 was expressed in Escherichia coli using a co-expression strategy with λ phosphatase, intended to reduce the potential toxicity associated with heterologous expression of an active eukaryotic kinase. The recombinant protein was then purified by nickel-affinity chromatography, first using a batch purification approach and subsequently using an automated chromatographic system, in order to obtain protein suitable for downstream activity assays.

A second objective of the work was to develop and optimize an enzymatic assay for CDKL1 activity. Since no standard biochemical assay for CDKL1 was available in the laboratory, different peptide substrates were tested using the ADP-Glo™ kinase assay, which indirectly measures kinase activity through the quantification of ADP generated during ATP-dependent phosphorylation. Reaction parameters were then optimized, including substrate selection, reaction time, pH, buffer composition and ATP concentration. This optimization was necessary to define reproducible assay conditions allowing quantitative evaluation of CDKL1 catalytic activity.

Finally, the optimized assay was used to perform a preliminary analysis of CDKL1 inhibition by selected compounds. Particular attention was given to punicalagin and structurally related ellagitannins, based on previous kinase-screening data indicating that CDKL1 may represent one of the potential targets of these molecules. Although punicalagin and related compounds had already been identified as potent inhibitors of other kinases, including SGK1 and SGK2, their activity toward CDKL1 had not been biochemically characterized in this experimental system. The final objective of the thesis was therefore to evaluate whether CDKL1 can be directly inhibited by these compounds and to provide a first biochemical basis for future studies aimed at understanding their mechanism of action, selectivity profile and possible structural interaction with the kinase domain of CDKL1.

Overall, this work was designed as a preliminary but necessary step toward the biochemical characterization of CDKL1 as an understudied human kinase and as a possible molecular target of natural polyphenolic compounds.

3. Materials and methods

3.1. E. Coli transformation

Although bacteria possess endogenous protein kinases and phosphatases, their phosphorylation networks are considerably less complex than those of eukaryotic cells. Consequently, heterologous expression of a eukaryotic protein kinase in Escherichia coli may result in extensive non-physiological phosphorylation of endogenous bacterial proteins. This aberrant phosphorylation can alter protein structure, stability, solubility, and activity, ultimately impairing bacterial growth and, in some cases, causing severe cellular toxicity. As a result, bacterial expression of many eukaryotic protein kinases can be challenging, often making alternative expression systems or phosphatase co-expression strategies preferable.

Co-expression of an exogenous protein phosphatase provides an effective means of mitigating these effects by reversing promiscuous phosphorylation of bacterial proteins and helping to preserve proteome homeostasis. Using this approach, Albanese and co-workers systematically evaluated the bacterial expression of a panel of human serine/threonine and tyrosine protein kinases(31). Among the kinases tested, CDKL1 was identified as being suitable for recombinant expression under these conditions. Therefore, recombinant CDKL1 was produced according to the strategy described by Albanese et al. 2018. Briefly, E. coli cells were co-transformed with a plasmid encoding CDKL1 and a second plasmid expressing the bacteriophage λ protein phosphatase (λPP), a Mn^{2+}-dependent phosphatase that efficiently dephosphorylates phosphoserine and phosphothreonine residues and, with lower efficiency, phosphotyrosine residues. By counteracting the accumulation of aberrantly phosphorylated bacterial proteins, λPP reduces the toxicity associated with ectopic kinase activity and improves recombinant protein production.

3.2. Purification

The recombinant CDKL1 construct was designed with an N-terminal 6×His tag to enable purification by immobilized metal affinity chromatography (IMAC). This purification strategy exploits the high affinity of histidine residues for immobilized nickel ions, allowing selective retention of the recombinant protein while most bacterial proteins are removed during the washing steps. As an initial approach, CDKL1 purification was performed using a batch protocol with Ni-NTA resin.

Following bacterial lysis and clarification of the soluble fraction by centrifugation, the protein extract was incubated overnight at 4 °C with equilibrated nickel affinity resin under constant agitation to maximize the interaction between the His-tagged recombinant protein and the resin. After the binding step, the resin was subjected to three consecutive washes with equilibration buffer to remove proteins that were either unbound or only weakly associated with the nickel matrix. Finally, bound proteins were eluted by incubating the resin with buffers (Table 3) containing progressively higher concentrations of imidazole. Since imidazole competes with histidine residues for nickel binding, the increasing concentration results in the sequential release of proteins according to their affinity for the resin. Four eluate fractions were collected and analyzed together with the initial lysate, the flow-through and the wash fractions by SDS-PAGE.

Table 3. Purification buffers composition.

LYSIS BUFFER	EQ-BUFFER Ni-NTA	DILUTION BUFFER	ELUTION BUFFER 3 Ni
50mM KPO4 pH 7.4	50mM KPO_4 pH 7.4	50mM KPO_4 pH 7.4	50mM KPO_4 pH 7.4
500mM NaCl	150mM NaCl	10% glycerol	150mM NaCl
10% glycerol	10% glycerol	10mM imidazole	10% glycerol
0.05% NP40	10mM imidazole		500mM imidazole

The concentration of the eluted and purified protein was measured by Beauford reaction. The quality and purity were verified via SDS-PAGE. Most of the CDKL1 proteins were successfully obtained with minor impurities that can be observed in the SDS gel.

As the eluted protein was obtained in a buffer containing high concentrations of imidazole, buffer exchange was required prior to downstream activity assays. This was performed using a 10 kDa molecular weight cut-off Amicon centrifugal filter unit. The sample was loaded into the device to approximately half of its maximum capacity, and an equivalent volume of the *desired buffer* was added. The sample was then subjected to repeated centrifugation steps to progressively replace the original buffer. Centrifugation was carried out at 3,000–12,000 rpm for 12–15 min per cycle, with the filtrate discarded after each step and approximately 15 mL of fresh buffer added. Once the final volume and buffer composition were achieved, the sample was aliquoted and frozen in liquid nitrogen until further use in enzymatic assays.

3.3. Finding optimal conditions for CDKL1

Kinase activity was quantified using the ADP-Glo™ assay, an indirect luminescence-based method that measures ADP production. This approach was selected over radioactive assays due to its safety and operational convenience, while maintaining high sensitivity for ATP-dependent enzymes such as kinases. The assay consists of two sequential steps following completion of the enzymatic reaction.

Upon completion of the kinase reaction, an equal volume of ADP-Glo™ reagent was added to each sample to terminate the reaction and deplete any remaining ATP not converted into ADP. Samples were incubated for 40 minutes under these conditions. Subsequently, the Kinase Detection Reagent was added, converting ADP into ATP, which is then quantified via a luciferase-mediated bioluminescent reaction, generating a stable luminescent signal. This step was incubated for at least 30 minutes, with samples protected from light.

The resulting bioluminescent signal was measured using an automated plate reader (ADP-GloMax) and reported as relative light units (RLU), which are directly proportional to kinase activity. All reagents were provided as part of the ADP-Glo™ assay kit, including the ADP-Glo™ Reagent (ready to use), the Detection Reagent (diluted prior to use), and ultra-pure ATP (10 mM).

All enzymatic assays were performed in 1.5 mL Eppendorf LoBind tubes to minimize adsorption of enzymes and substrate to the tube surface and ensure reagent availability during the reaction. Peptide substrates and reaction conditions were optimized to determine the most suitable assay parameters.

3.3.1. Buffers

In order to enable accurate investigation of CDKL1 kinase activity assays were first optimized by systematically evaluating key experimental parameters pH, buffer composition, ATP concentration, and substrate concentration. Buffers used to do these experiments were:

Table 4. Buffers used during conditions optimization.

Buffer used	Buffer composition	Assays
KPO_4 40 mM ph 8	4.8 mg/mL BSA 4.8% glycerol 10mM $MgCl_2$ H_2O at volume	Substrate and ATP titration Substrate screening Time-course
TrisHCl 40 mM pH 7,5	4.8 mg/mL BSA 4.8% glycerol 10mM $MgCl_2$ H_2O at volume	Substrate screening
NaPO4 6x	BSA 4.8mg/ml Glycerol 4.8% MgCl2 10mM H_2O at volume	pH

3.3.2. Reaction conditions

Each assay contained mixes with different reaction conditions, these mixes contained reaction buffer, NP-40 0.026%, DTT 1M, $MgCl_2$ 200 mM and H_2O for a final volume. Conditions varied according to the test and therefore there were additions to this mix.

Table 5. Reaction conditions for each assay.

Assay	Conditions	Annotations
Substrate screening	Buffer: KPO_4 / TrisHCl Additions to mix: CDKL1 8 µM, ATP 1 mM	Blank tubes contain buffer instead of CDKL1. Buffers differed among assays. Each substrate was tested at two concentrations 25 µM and 75 µM.
Substrate titration	Buffer: KPO_4 Additions to mix: CDKL1 8 µM,	Blank tubes contain buffer instead of CDKL1.

	ATP 1 mM	
Time course	Buffer: KPO_4 Additions to mix: ATP 1 mM, CDKL1 8 μM and CDKL1-3 340 μM	Blank tubes contain buffer instead of CDKL1. Aliquots from reaction were collected at 0, 5, 10, 20, 30, 50, and 60 min.
pH	Buffer: NaPO4 6x Additions to mix: ATP 1 mM	Different mixes were prepared varying buffer pH. CDKL1 100 uM and CDKL1-3 340 μM were added to tubes.
ATP titration	Buffer: KPO_4 Additions to mix: CDKL1 8 μM and CDKL1-3 340 μM	ATP concentrations used were 8mM, 4mM, 2mM, 1mM, 500 μM, 250 μM and 100 μM.

Buffer conditions

Reaction mixtures were prepared with identical components, varying only the buffer composition; buffers used were KPO4 40mM 6X, KPO4 20mM 6X, TRIS pH 6.5 6X and Hepes & NaCl 6X. CDKL1 100 uM and CDKL1-3 340 μM were added to tubes.

All enzymatic reactions were incubated at 30 °C for 15 min, then immediately 10 μL of ADP-Glo™ reagent were added to terminate the reaction. The ADP-Glo™ reagent was incubated for 35 min, followed by incubation with the Detection Reagent for 60 min prior to luminescence measurement. ADP-Glo™ assay steps were performed at 23 °C using a thermoblock.

Kinetic analyses were performed to characterize CDKL1 enzymatic activity. The maximum reaction velocity (Vmax) and the Michaelis constant (Km) were determined using GraphPad Prism (GraphPad Software, San Diego, CA, USA) by fitting experimental data to the Michaelis–Menten model. Vmax represents the maximal catalytic rate achieved by the enzyme under saturating substrate conditions, reflecting the turnover capacity of CDKL1 when all active sites are fully occupied. In contrast, Km corresponds to the substrate concentration at which the reaction velocity reaches half of Vmax and is commonly used as an indicator of substrate affinity. Lower Km values suggest higher affinity between the enzyme and substrate, whereas higher Km values indicate weaker substrate binding.

Together, these parameters provide insight into the catalytic efficiency of CDKL1 and its interaction with the substrate under the assay conditions employed. In particular, the relationship between Km and substrate concentration is critical for defining appropriate experimental conditions, as measurements performed near the Km value allow for greater sensitivity to changes in enzymatic activity. Given that CDKL1 is an ATP-dependent kinase, kinetic parameters were determined with consideration of ATP concentration, as ATP acts as a co-substrate and may influence both catalytic activity and apparent kinetic constants. These analyses established a quantitative framework for defining optimal assay conditions and for supporting subsequent inhibition studies.

3.3. Inhibitors study

All compounds evaluated as CDKL1 inhibitors were dissolved at 10mM in DMSO (stock).
Inhibition assays were performed as follow: 40 mM Tris-HCl pH 7.5, 20 mM $MgCl_2$, 1 mM DTT, 0.1 mg/mL BSA, 0.026% NP-40, 750 µM CDKL1-3 peptide substrate, 144 µM CDKL1 was incubated 5' at room temperature together with the investigated inhibitor or DMSO as control. Reaction was initiated by adding ATP (3 mM) to a final volume of 10 µL.

The reaction proceeded for 10 minutes at 30 °C. Subsequently, ADP-Glo™ reagent was added and incubated for 30 minutes, followed by a 50-minute incubation with the Detection Reagent, both steps being carried out at 23 °C.

For compounds confirmed as inhibitors in preliminary screening, dose–response experiments were performed to determine the half-maximal inhibitory dose (ID_{50}), defined as the inhibitor concentration required to reduce enzymatic activity by 50%. ID_{50} values were determined using nonlinear regression analysis in GraphPad Prism. Data were fitted to the equation:

$$Y = \frac{V}{1 + \left(\frac{X}{\mathrm{ID}_{50}}\right)} \qquad [1]$$

where Y represents the observed enzymatic activity, V corresponds to maximal activity in the absence of inhibitor, and X is the inhibitor concentration.

In addition to ID_{50} determination, inhibition constants (Ki) were determined using the Morrison equation, which is appropriate for tight-binding inhibitors, where inhibitor concentration is comparable to enzyme concentration. Under these conditions, classical Michaelis–Menten assumptions are not valid, and inhibitor depletion must be considered. The Morrison equation describes the fractional inhibition of enzyme activity as:

$$v = v_0\left(1-\frac{([E]_t + [I]_t + K_i) - \sqrt{([E]_t + [I]_t + K_i)^2 - 4[E]_t[I]_t}}{2[E]_t}\right) \qquad [2]$$

where v is the observed reaction velocity, v_0 is the velocity in the absence of inhibitor, $[E]_t$is the total enzyme concentration, $[I]_t$is the total inhibitor concentration, and Ki is the inhibition constant. This model accounts for the formation of a tight enzyme–inhibitor complex and provides a more accurate estimation of inhibitory potency under conditions where inhibitor binding significantly reduces the concentration of free enzyme. Lower Ki values indicate stronger binding and therefore greater inhibitory effectiveness, whereas higher Ki values are consistent with weaker interaction and reduced potency.

In addition, the calculation of Ki values considered the characteristic kinetic parameters of ATP, given that CDKL1 is an ATP-dependent kinase and inhibitor binding may be influenced by competition with ATP at the catalytic site.

4. Results and Discussion

4.1. *E. Coli* transformation and protein expression

Although bacteria possess endogenous protein kinases and phosphatases, their phosphorylation networks are considerably less complex than those of eukaryotic cells. Consequently, heterologous expression of a eukaryotic protein kinase in Escherichia coli may result in extensive non-physiological phosphorylation of endogenous bacterial proteins. This aberrant phosphorylation can alter protein structure, stability, solubility, and activity, ultimately impairing bacterial growth and, in some cases, causing severe cellular toxicity. As a result, bacterial expression of many eukaryotic protein kinases can be challenging, often making alternative expression systems or phosphatase co-expression strategies preferable.

Co-expression of an exogenous protein phosphatase provides an effective means of mitigating these effects by reversing promiscuous phosphorylation of bacterial proteins and helping to preserve proteome homeostasis. Using this approach, Albanese (42)and co-workers systematically evaluated the bacterial expression of a panel of human serine/threonine and tyrosine protein kinases. Among the kinases tested, CDKL1 was identified as being suitable for recombinant expression under these conditions. Therefore, recombinant CDKL1 was produced according to the strategy described by Albanese *et al (42).* Briefly, E. coli cells were co-transformed with a plasmid encoding CDKL1 and a second plasmid expressing the bacteriophage λ protein phosphatase (λPP), a Mn^{2+}-dependent phosphatase that efficiently dephosphorylates phosphoserine and phosphothreonine residues and, with lower efficiency, phosphotyrosine residues. By counteracting the accumulation of aberrantly phosphorylated bacterial proteins, λPP reduces the toxicity associated with ectopic kinase activity and improves recombinant protein production.

Transformation efficiency was evaluated running cell extracts in SDS page, comparing pre- and post-induced results. Protein expression was initially induced with several quantities of IPTG, 0.1mM, 0.5mM and 1mM. Experiments showed that induction with 0,5mM IPTG was the most effective condition. A prominent protein band was observed following induction, migrating just below the 37 kDa marker, consistent with the expected molecular weight of recombinant CDKL1 (35.25 kDa). (Fig. 6)

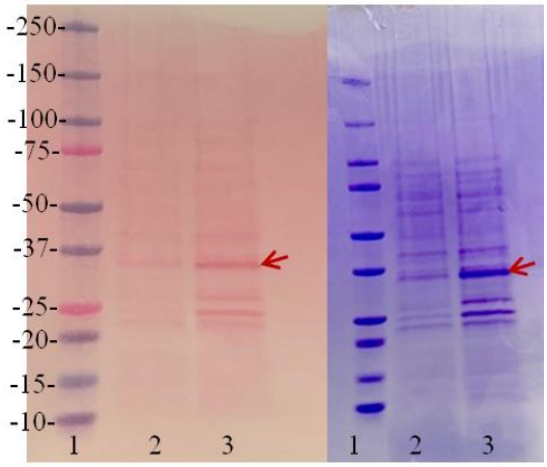

Figure 6. CDKL1 induction. The same samples were loaded on SDS-page gel colored with coomasie brilliant blue (left panel) or transferred on a membrane and colored with ponceaux solution (right panel). Lane 1 corresponds to molecular markers, while lanes 2 and 3 correspond to samples pre- and post-induced, respectively.

4.2. Purification

Protein purification was performed using both batch affinity purification and high-performance liquid chromatography (HPLC)-based purification methods. In both cases, the purified protein samples were subsequently subjected to buffer exchange to remove imidazole and transfer the protein into a suitable assay-compatible buffer. This step was necessary to eliminate potential interference of imidazole with downstream kinase activity assays.

Batch purification provides a rapid and straightforward approach, allowing efficient enrichment of the target protein with minimal handling steps. However, this method may result in lower purity due to co-elution of non-specifically bound proteins. In contrast, HPLC-based purification offers higher resolution and improved separation efficiency, leading to enhanced sample purity and better removal of contaminants.

Electrophoretic analysis was performed on samples obtained from both purification methods to assess protein purity and detect potential contaminants. No substantial differences in purity were observed between batch- and HPLC-purified samples. However, a higher protein concentration was consistently obtained in samples purified by HPLC.

Given that washing conditions were comparable between the two purification strategies, the observed difference in yield is unlikely to result from the purification process itself. Instead, it may reflect variability in upstream factors, such as differences in protein expression efficiency in *E. coli*.

4.2.1. Batch purification

CDKL1 proteins were purified from Escherichia coli cell pellets according to protocols established by Albanese *et al*.(42). The electrophoretic analysis of the purification process is shown in Figure 7. A prominent protein band corresponding to the expected molecular weight of recombinant CDKL1 (~35.3 kDa) was readily detected in the bacterial lysate after induction, confirming successful recombinant expression. Following incubation with the Ni-NTA resin, only a limited fraction of CDKL1 remained in

the flow-through, indicating that most of the recombinant protein efficiently bound to the affinity matrix. Likewise, relatively small amounts of CDKL1 were detected in the wash fractions, suggesting that the interaction between the His-tag and the nickel resin was sufficiently stable to withstand the washing procedure.

As expected, the highest enrichment of CDKL1 was observed in the elution fractions, where the intensity of the band at the expected molecular weight increased markedly compared with the starting lysate. Most of the recombinant protein was recovered within the first elution fractions, while only minor amounts were released in the subsequent eluates, indicating that most resin-bound CDKL1 was efficiently recovered under the selected elution conditions.

Although the purification resulted in a substantial enrichment of recombinant CDKL1, several additional protein bands were still visible in the elution fractions, indicating the co-purification of endogenous *E. coli* proteins. Such contaminants are commonly observed after a single IMAC purification step, as some bacterial proteins either contain exposed histidine-rich regions or interact non-specifically with the nickel resin. Nevertheless, these contaminating proteins were considerably less abundant than CDKL1, demonstrating that the batch purification protocol successfully enriched the recombinant kinase from the bacterial lysate.

Overall, the batch IMAC protocol successfully enriched recombinant CDKL1 from the bacterial lysate, demonstrating that the His-tag was fully functional and that the protein could be efficiently captured by the nickel resin. Nevertheless, the persistence of several contaminating proteins in the elution fractions suggested that the purification conditions could be further optimized. Therefore, the affinity purification was repeated using an automated FPLC/FPLCsystem, which allows tighter control of the chromatographic parameters and enables a more accurate evaluation of protein recovery and purity.

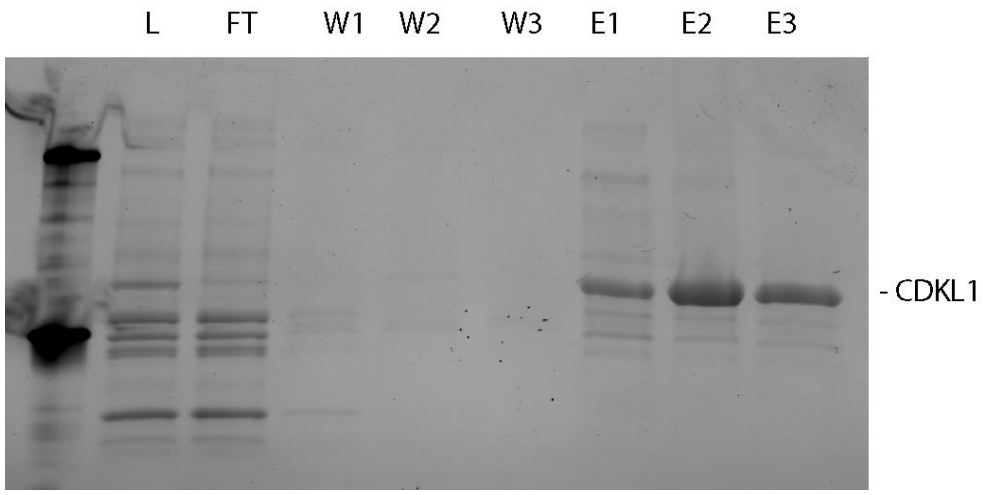

Figure 7. Batch purification. Lane 1 corresponds to molecular markers, from left to right there is lysate (L), flow through (FT), washes 1 to 3 (W1, W2, and W3, respectively), and eluates 1 to 3 (E1, E2, and E3, respectively).

Protein concentration was determined using the Bradford assay, with a bovine serum albumin (BSA) standard curve (10, 5, 2.5, 1.25, 0.6, and 0 mg/mL). Absorbance was measured at 600 nm using a GloMax plate reader with a transparent plate. Eluates had an average concentration of CDKL1 of 116 μM/ μL.

4.2.2. FPLC purification

FPLC purification was performed using an ÄKTA Start system equipped with a 1 mL Ni–NTA affinity column. The column was equilibrated with 15 mL of equilibration buffer at a flow rate of 1 mL/min prior to sample loading. The protein sample (60–70 mL) was then applied to the column at a flow rate of 0.5 mL/min. Following system setup, the purification process was carried out under automated conditions using the ÄKTA Start system. The resulting chromatographic profile is shown in Figure 8.

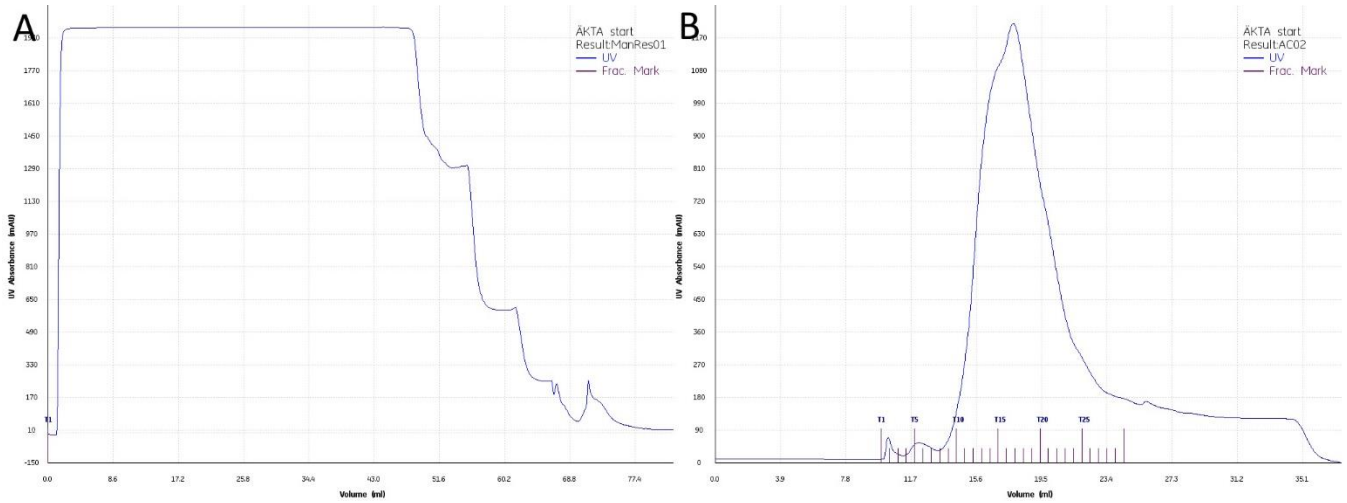

Figure 8. FPLC purification. Chromatogram profile, A corresponds to column washing after sample injection while B represents elution phase.

Elution was carried out using elution buffer 3 (Ni) over a 15 mL gradient, yielding approximately 30 fractions of 0.5–1 mL each. Three fractions were obtained containing tubes from 4 to 6 (E1), 9 to 25 (E2) and 26 to 30 (E3). Purification quality was assessed by gel electrophoresis afterwards, confronting the sample, the flow through, the washes (1 and 2), the eluates (E1-E3), and the sample post-buffer exchange. As expected, CDKL1 bands were present in all eluates, but it was visibly more concentrated on E2, we also confirmed that buffer exchange was able to maintain a big portion of the protein. (Fig. 9)

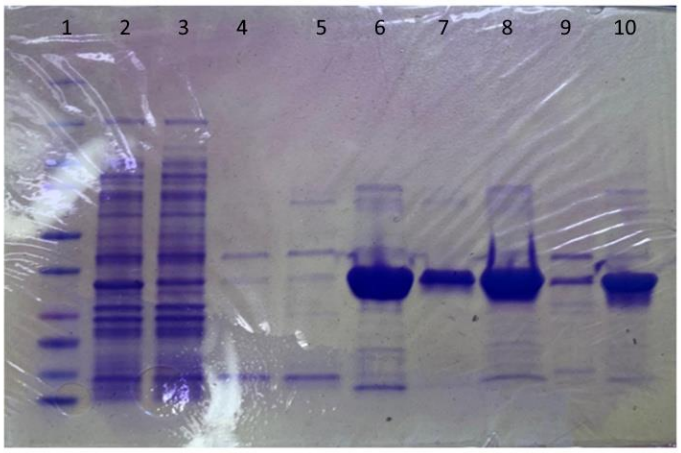

Figure 9. CDKL1 purification by FPLC. FPLC purification was made and then electrophoresis was prepared to evaluate it. SDS-page gel was stained with Coomasie Blue reagent. Aliquotes were taken from washes 1 and 2, eluates and sample after buffer exchange. Lane 1 corresponds to molecular markers, lane 2 contains the injected sample, lane 3 corresponds to flow through, at lane 4 is wash 1 and lane 5 has wash 2, lane 6 contains eluate 2, lane 7 is eluate 3, lane 8 corresponds to the sample post-buffer exchange, lane 9 contains eluate 1 and lane 10 contains the sample post-buffer exchange at half concentration.

Protein concentration was determined using the Bradford assay, with a bovine serum albumin (BSA) standard curve (10, 5, 2.5, 1.25, 0.6, and 0 mg/mL). Absorbance was measured at 600 nm using a GloMax plate reader with a transparent plate. After buffer exchange, the sample was 3mL, buffer was added until total volume was 6mL in order to obtain a sample with an average concentration of 17,5 mM + 5% glycerol. Then the sample was centrifugated at 12800 rpm, during 3' at 4°C.

4.3. Finding optimal conditions for CDKL1

In order to enable accurate investigation of CDKL1 kinase activity assays were first optimized by systematically evaluating key experimental parameters, including pH, buffer composition, ATP concentration, and substrate concentration. Kinetic analyses were subsequently performed to determine appropriate ATP and substrate concentrations, providing a quantitative basis for the selection of assay conditions applied to evaluate the inhibitory effects of selected compounds.

4.3.1. Substrate titration

Substrate screening was performed to identify the most suitable peptide for subsequent in vitro CDKL1 activity assays. The candidate substrates evaluated in this study are listed in Table 6.

Table 6. Sequences of peptide substrates.

Substrate ID	Sequence	Source
CDKL1-0	RPRSPGARR	Canning et al. 2018
CDKL1-1	TPARRPPSPRRSHHP	Johnson et al. 2022
CDKL1-2	STRRRPKTPLGKRDI	Johnson et al. 2022
CDKL1-3	RWGPRPGSSRRGIPP	Johnson et al. 2022
CDKL1-4	AKSPAPKSPVK	Yen et al. 1995
CDKL1-5	PKSGDRSGYSSPGSPGTPG	Yen et al. 1995
CDKL1-6	SKIGSTENLK	Yen et al. 1995

Peptides were selected based on three sources: the computational substrate predictions reported by Johnson et al. (2022)(43) and two experimental works. The first one is from Yen et al. (1995)(25), which investigated CDKL1 kinase activity on selected peptide substrates. The second work is from Canning et al. (2018)(20), which was able to elucidate the crystal structure of CDKL1-3 and CDKL5.

Johnson et al. used computational approaches to predict potential CDKL1 substrates by matching phosphoproteomic sites to the kinase sequence-preference motif(43). Although these predictions provide a useful starting point, they require experimental validation to determine whether the predicted sequences can be efficiently phosphorylated by CDKL1 under defined in vitro assay conditions. Therefore, peptide sequences showing the highest degree of agreement with the predicted CDKL1 substrate motif were selected. In particular, sequences corresponding to the 100th percentile match were considered (Figure 10A), and from these a consensus motif was derived (Figure 10B). This motif guided the design of the initial set of candidate substrates, corresponding to peptides 0–3.

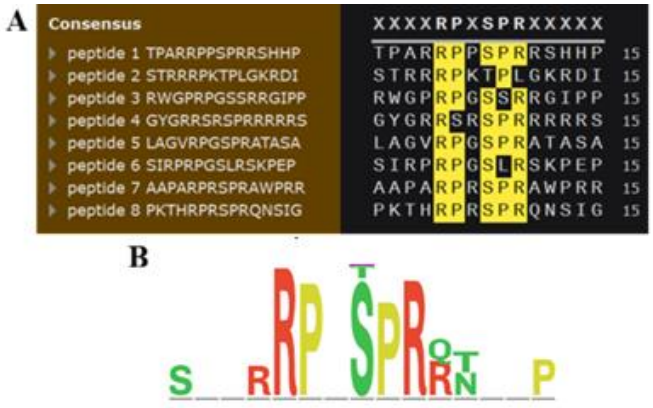

Figure 10. A Best predicted substrate peptides; B Best peptide substrate consensus sequence.

Additional peptides were selected based on the study by Yen et al. (1995), which examined the possible involvement of CDKL1, previously referred to as KKIALRE, in Alzheimer's disease. Although that study concluded that CDKL1 is unlikely to play a direct role in Alzheimer's pathology, it provided relevant experimental information on CDKL1 kinase activity and substrate phosphorylation(25). Two of the peptides described in that work, AKSPAPKSPVK and PKSGDRSGYSSPGSPGTPG, contain the X-Ser-Pro-X motif, characterized by a serine residue immediately followed by proline. This sequence arrangement is typical of substrates recognized by proline-directed serine/threonine kinases. Using these peptides, Yen et al. showed that CDKL1 displays properties consistent with proline-directed kinase activity, supporting its classification within this group.

A third peptide from the same study, SKIGSTENLK, lacks a proline residue adjacent to the phosphorylatable serine. Its inclusion is therefore informative because phosphorylation of this peptide would suggest that CDKL1 substrate recognition may not be strictly limited to canonical Ser/Thr-Pro motifs. These peptides were included in the present screening to further investigate CDKL1 substrate specificity and to compare computationally predicted substrates with peptides previously used in experimental kinase assays(25).

Due to the number of candidate substrates and experimental constraints, the substrate screening was performed across multiple assays runs. The corresponding results are shown in Figure 11. Peptides 0–3 were initially evaluated based on their availability. Among these, peptide 3 produced the highest level of enzymatic activity and was therefore selected as the reference substrate for subsequent comparisons (Figure 11A). Peptides 4–6 were then tested in later experiments and directly compared with peptide 3 under the same assay conditions (Figure 11B,C). In these assays, peptides 4–6 showed markedly lower phosphorylation levels than peptide 3.

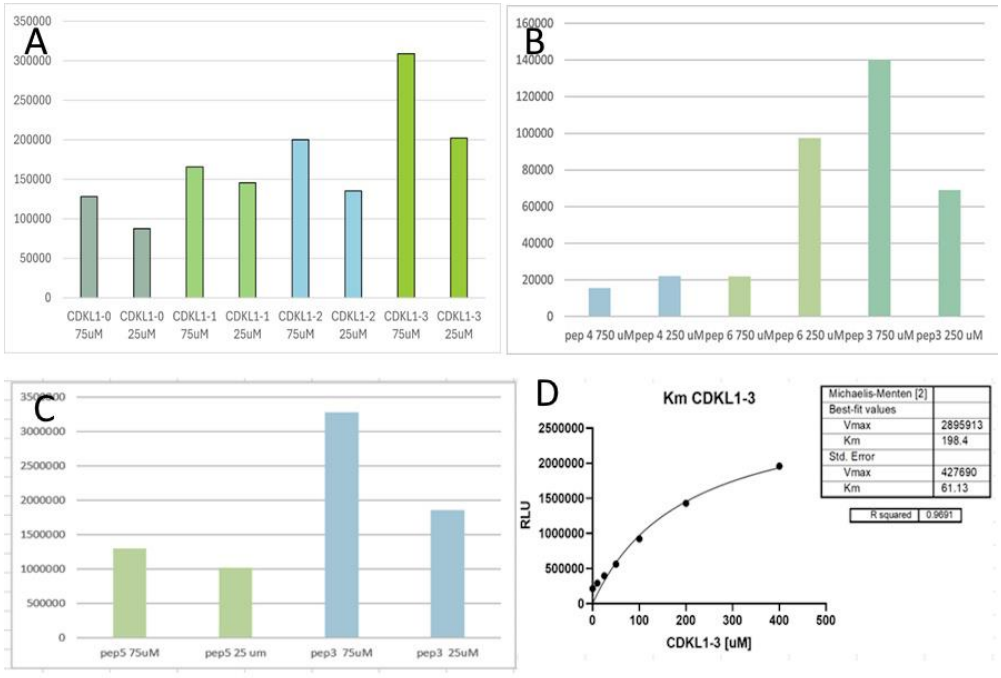

Figure 10. Peptide assays with the different candidates. A. Enzymatic assay comparing substrates 0-3. B. Comparison between peptide 3, 4 and 6. C. Comparison between peptide 3 and 5. D. Curve Michaelis-Menten of peptide 3.

The reduced activity observed with peptides 4–6 may reflect lower substrate compatibility with CDKL1, possibly due to differences in sequence recognition relative to the substrate-preference features predicted by Johnson *et al*.(43). Alternatively, technical factors such as peptide stability, solubility, or partial inactivation during storage and handling may also have contributed to the lower signal. Nevertheless, under the experimental conditions used in this study, peptide 3 consistently supported the highest CDKL1-dependent activity.

4.3.2. Reaction time

To identify an appropriate incubation time for CDKL1 activity assays, time-course experiments were performed across a range of reaction durations (5–60 minutes).

Analysis of the reaction curve (Figure 12) indicated that enzymatic activity increased linearly during the initial phase of the reaction, slowly approaching a plateau at longer incubation times indicating that measurements beyond this time point deviate from initial rate conditions. Optimal assay performance was observed at approximately 15 minutes, which was therefore selected as the standard incubation time for all subsequent experiments.

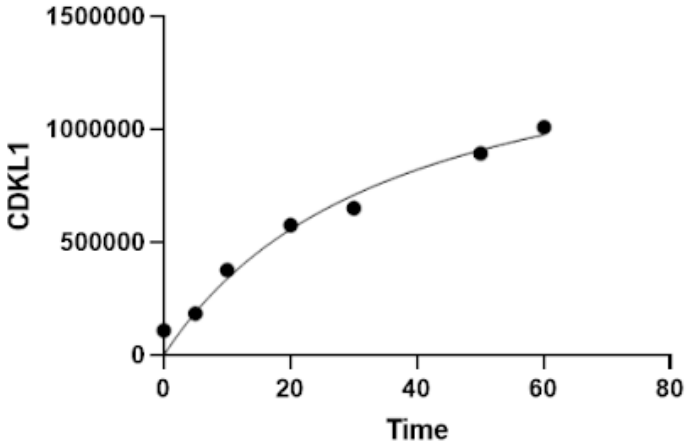

Figure 11. Time course assay. *CDKL1 activity is plotted toward reaction time [min]*

4.3.3. pH

The effect of pH on CDKL1 activity was evaluated across a range of conditions (pH 6.5–8.0) selected to remain within physiologically relevant limits. The resulting activity profiles are presented in Figure 13.

CDKL1 displayed a clear dependence on pH, with maximal activity observed under mildly acidic conditions. In particular, enzymatic activity was highest at pH 6.5 and decreased progressively to higher pH values. This trend indicates that slight variations in protonation state may influence catalytic efficiency or substrate interaction. Based on these observations, pH 6.5 was selected for all subsequent assays.

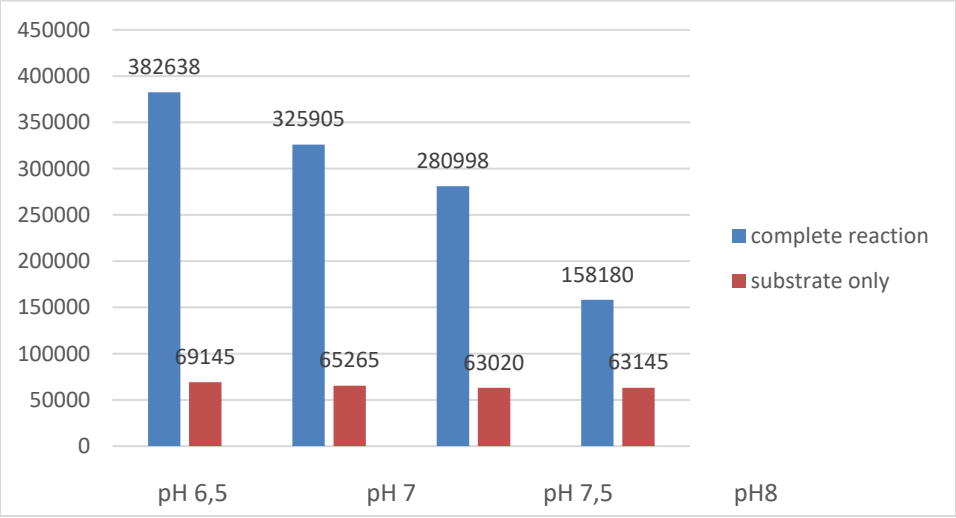

Figure 13. CDKL1 activity depending on pH. Blue bars ***represent*** CDKL1 activity at indicated pH. Red bars represent CDKL1 activity in the absence of the substrate peptide.

4.3.4. Buffer

Because kinase activity can be strongly affected by the chemical environment of the reaction, different buffer systems were evaluated to identify conditions supporting optimal CDKL1 activity. The tested buffers differed not only in their buffering species and pH, but also in their ionic composition and expected ionic strength, parameters that may influence protein stability, substrate recognition, and electrostatic interactions during catalysis.

The buffer tested included KPO_4 (40 mM, 6×), KPO_4 (20 mM, 6×), Tris-HCl (pH 6.5, 6×), and HEPES with NaCl (6×). The resulting activity profiles are presented in Figure 14.

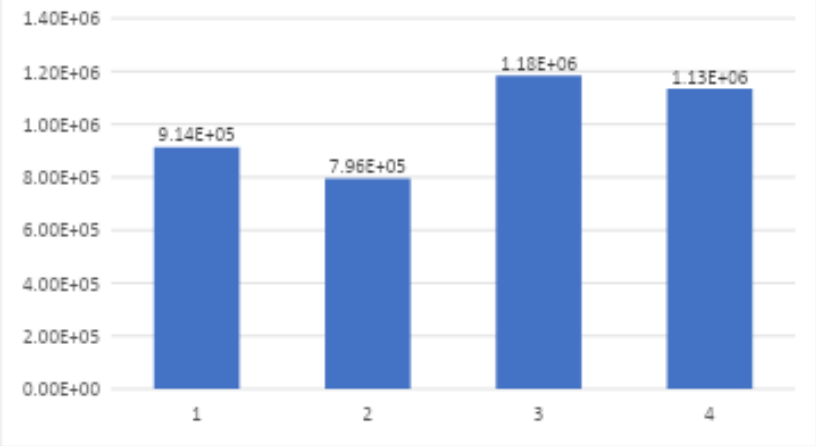

Figure 12. Effect of different buffers on CDKL1 activity. Buffers used were 1. KPO_4 (40 mM, 6×), 2. KPO_4 (20 mM, 6×), 3. Tris-HCl (pH 6.5, 6×), and 4. HEPES with NaCl (6×).

Among these conditions, Tris-HCl at pH 6.5 produced the highest enzymatic activity. This result is consistent with the pH optimization assay and suggests that CDKL1 activity is favored in a mildly acidic environment supported by this buffering system. Accordingly, Tris-HCl pH 6.5 was selected for all subsequent assays.

4.3.5. Substrates affinity

ATP titration experiments were performed to define a suitable ATP concentration for CDKL1 activity assays. This parameter was also relevant for subsequent inhibition studies, as many kinase inhibitors compete directly with ATP for binding to the catalytic pocket, or interact with residues located in or near the ATP-binding site, thus preventing productive ATP binding with the enzyme. Therefore, defining the apparent affinity of CDKL1 for ATP was essential to establish assay conditions suitable for evaluating the mechanism of action of potential inhibitors.

A range of ATP concentrations (12.5 µM, 25 µM, 50 µM, 100 µM, 200 µM, 400 µM, and 800 µM) was tested, and the resulting titration curve is shown in Figure 15. Analysis of these data yielded a Michaelis constant (Km) for ATP of 203.7 µM.

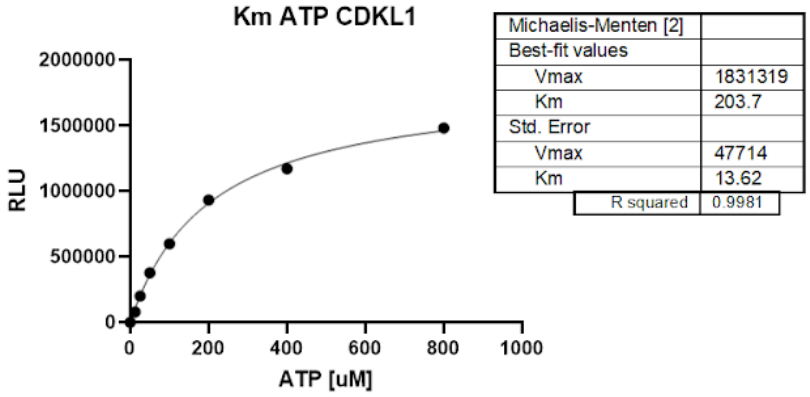

Figure 13. ATP titration curve.

This result indicates that, under the assay conditions used, CDKL1 displays a relatively low apparent affinity for ATP. For this reason, a concentration of 300 µM ATP was selected for subsequent assays, as it provides substrate levels above the Km while remaining within a range appropriate for reliable detection of enzymatic activity and inhibitor effects

4.4. Finding specific CDKL1 inhibitors

Given the limited biochemical characterization of CDKL1, inhibitor profiling was used to assess its susceptibility to small-molecule modulation and to obtain an initial pharmacological profile. In kinases, this approach is particularly informative because it can reveal compounds capable of interacting with the catalytic domain and provide indirect insight into the properties of the ATP-binding site.

Since CDKL1 has been associated with cancer-related processes such as proliferation, survival, and invasion, the identification of active inhibitors is relevant not only for its biochemical characterization, but also for future functional studies and the development of more selective CDKL1-targeting molecules.

4.4.1. Activity of known kinase inhibitors

To further define the inhibitor sensitivity profile of CDKL1, an initial screening was performed using compounds previously reported by Canning et al. (2018) to interact with this kinase(20). This approach allowed the identification of inhibitors capable of producing measurable effects on CDKL1 activity under the assay conditions employed. The inclusion of known kinase inhibitors also provided an important reference for comparison with the ellagitannins tested in this study. By evaluating both groups of compounds under the same experimental conditions, it was possible to assess whether the effects observed for ellagitannins were comparable to those of inhibitors with reported activity toward CDKL1, thereby strengthening the interpretation of their potential as CDKL1 modulators.

Canning et al. (2018) identified approximately 20 chemical compounds capable of stabilizing the CDKL1 kinase domain to different extents by thermal shift screening(20). Since thermal stabilization can indicate compound binding, some of these molecules were selected for functional inhibition assays. In particular, staurosporine and indirubin were chosen because they were among the strongest binders reported by Canning et al., whereas curcumin was selected as a compound with an intermediate stabilizing effect. These inhibitors were therefore used to compare binding data obtained by thermal shift analysis with the ability of the same compounds to reduce CDKL1 enzymatic activity in vitro

All of these compounds were initially evaluated at three concentrations: 100, 10, and 1 μM. The results are presented in Table 8. Staurosporine inhibited CDKL1 activity by 89% at 10 μM, while the other components required higher concentrations; both, indirubin and curcumin inhibited CDKL1 activity by 83% and 60%, respectively, at 100 μM, indicating a substantially weaker inhibitory effect. This trend is consistent with the thermal shift data reported by Canning et al., in which curcumin stabilized CDKL1 by 3.6 °C, while indirubin and staurosporine produced a larger shift around 6 °C. Taken together, these findings suggest that the extent of thermal stabilization may reflect, at least in part, the functional inhibitory capacity of these compounds toward CDKL1.

This ranking is consistent with the binding trend reported by Canning et al., in which indirubin exhibited a stronger stabilizing effect on CDKL1 than curcumin, although weaker than staurosporine. Taken together, these results further support the correspondence between thermal stabilization and functional inhibition observed for the compounds tested.

Table 8. Inhibition assay results.

Compound	Inhibition percentage
Curcumin 100 μM	58,88 ± 4,54 %
Curcumin 10 μM	11,58 ± 2,36 %
Curcumin 1 μM	1,94 ± 4,11 %
Staurosporine 100 μM	93,44 ± 5,04 %
Staurosporine 10 μM	88,84 ± 2,30 %
Staurosporine 1 μM	25,76 ± 3,88 %
CX4945 1 mM	28,55 ± 16,69
CX4945 100 μM	-29,84 ± 10,89
CX4945 10 μM	-32,69 ± 15,06
Indirubin 1 mM	82,81 ± 3,30
Indirubin 100 μM	14,48 ± 21,56
Indirubin 10 μM	-7,41 ± 12,76

Further analyses were carried out to determine the inhibitory potency of staurosporine and indirubin by estimating its inhibition potency. To this end, a dose–response assay was performed using a range of concentrations according to each inhibitor. Staurosporine concentrations were 6.25 µM, 12.5 µM, 25 µM, 50 µM, 100 µM, and 1 mM. Staurosporine is a well known ATP competitive, broad-spectrum inhibitor of both tyrosine and serine/threonine protein kinases(44,45). Therefore, the resulting data were fitted according to [2] model (see materials and Methods, section 3.3) to calculate the affinity constant Ki, that resulted of 0.24 µM (Figure 16). This low micromolar value is consistent with high inhibitory potency and supports the classification of staurosporine as a strong, yet not selective, inhibitor of CDKL1 under the assay conditions employed.

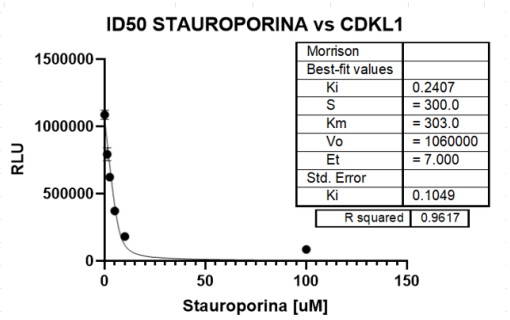

Figure 14. Dose-response curve of CDKL1 inhibition by Staurosporine.

On the other hand, as indirubin had a weaker response, the range of concentrations used was different, 50 µM, 100 µM, 200 µM, 300 µM, 500 µM, and 1 mM. The resulting data were used to generate a titration curve, shown in Figure 17. Analysis of this curve yielded an inhibition constant (Ki) of 1.4 µ M, indicating a weaker interaction with CDKL1 compared with staurosporine, although still consistent with measurable inhibitory activity under the assay conditions employed.

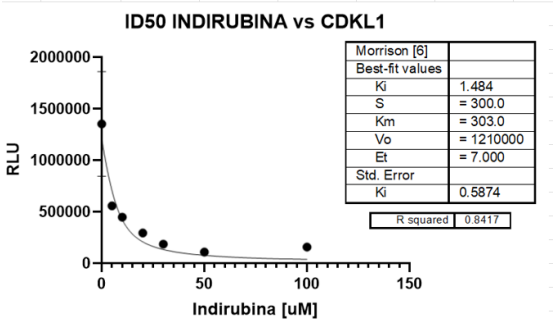

Figure 15. Dose-response curve of CDKL1 inhibition by indirubin.

4.4.2. Evaluation of new CDKL1 inhibitors

In previous experiments, punicalagin was evaluated externally using the Eurofins KinomeScan platform, which provides broad profiling of compound interactions across the kinome. This analysis showed that punicalagin affected several kinases with different degrees of potency. Among the kinases included in the panel, CDKL1 and CDKL5 were among the most sensitive, with 50 μM punicalagin causing an almost complete reduction of kinase activity.

Based on these observations, we decided to further investigate the inhibitory activity of punicalagin against CDKL1 and to extend the analysis to other ellagitannins (ETs). Four compounds were therefore evaluated in the initial screening: punicalagin, chebulagic acid, vescalagin, and ellagic acid. The compounds were tested at selected concentrations, and the results are presented in Table 10.

Overall, the four ellagitannins showed different degrees of inhibition of CDKL1 activity. At 100 μM, punicalagin inhibited CDKL1 activity by approximately 68%, whereas ellagic acid reduced CDKL1 activity by approximately 65%. Chebulagic acid and vescalagin showed stronger inhibitory effects, both reaching nearly complete inhibition at 100 μM. Vescalagin also showed marked inhibition at 1 μM, reducing CDKL1 activity by approximately 36%, suggesting a concentration-dependent effect already detectable at low micromolar concentration.

These results identified chebulagic acid and vescalagin as the most active ellagitannins under the assay conditions employed and therefore justified their selection for further characterization. To define their inhibitory potency more precisely, both compounds were subsequently analyzed by dose-response experiments over a broader concentration range. The resulting titration curves are shown in Figure 18. Analysis of these curves yielded apparent inhibitory constants of 4.3 μM for chebulagic acid and 2.4 μM for vescalagin. These values indicate potent inhibition of CDKL1 activity under the assay conditions employed and place both compounds among the most active inhibitors identified in this study. In particular, vescalagin showed an apparent inhibitory potency in the same range as that observed for indirubin, used here as a reference kinase inhibitor.

It should be noted that the inhibitory potency determined in our in vitro titration assays was lower than expected based on the initial KinomeScan data obtained with punicalagin. This discrepancy may be explained, at least in part, by differences in assay format, kinase construct, substrate, ATP concentration, detection method, and experimental conditions. Nevertheless, despite these quantitative differences, the results obtained in our assay confirmed that several ellagitannins are able to inhibit CDKL1 activity, with chebulagic acid and vescalagin emerging as the most active compounds in this series.

All ellagitannin-derived inhibitors were initially evaluated at two concentrations, 100 and 10 μM. The results are presented in Table X. Vescalagin displayed a marked concentration-dependent inhibitory effect, reducing CDKL1 activity by approximately 36% at 1 μM and reaching nearly complete inhibition at 100 μM, chebulagic acid produced about 95% inhibition at the same concentration. Punicalagin and ellagic acid had a marked difference at 100 μM, inhibiting only around 68% and 65%, respectively, indicating a weaker inhibitory effect under the same experimental conditions. These findings identified vescalagin and chebulagic acid as the more active compounds and justified their selection for further characterization.

Table 10. Experimental inhibitors test results.

Compound	Inhibition percentage
Punicalagin 100 μM	67,97 ± 28,17 %
Punicalagin 1 μM	14,21 ± 4,87 %
Chebulagic acid 100 μM	94,49 ± 1,02 %
Chebulagic acid 1 μM	7,16 ± 0,78 %
Vescalagin 100 μM	118,23 ± 2,44
Vescalagin 1 μM	25,75 ± 14,19
Ellagic acid 100 μM	65,02 ± 6,67
Ellagic acid 1 μM	11,11 ± 5,15

To define its inhibitory potency more precisely, chebulagic acid and vescalagin were subsequently tested; they had a similar curve which is why the concentration range was similar (1 µM, 2,5 µM, 5 µM, 10 µM, 25 µM, 50 µM, and 100 µM. Vescalagin had an additional point at 7,5 µM and 20 µM instead of 25 µM. The results are summarized in figure 18 for vescalagin and chebulagic acid. Analysis of these data yielded a Ki value of 4.3 µM for chebulagic acid while 2,5 µM for vescalagin, positioning vescalagin over chebulagic acid. In terms of inhibitory strength, this places vescalagin among the most active compounds identified in this study, with potency comparable to that observed for staurosporine.

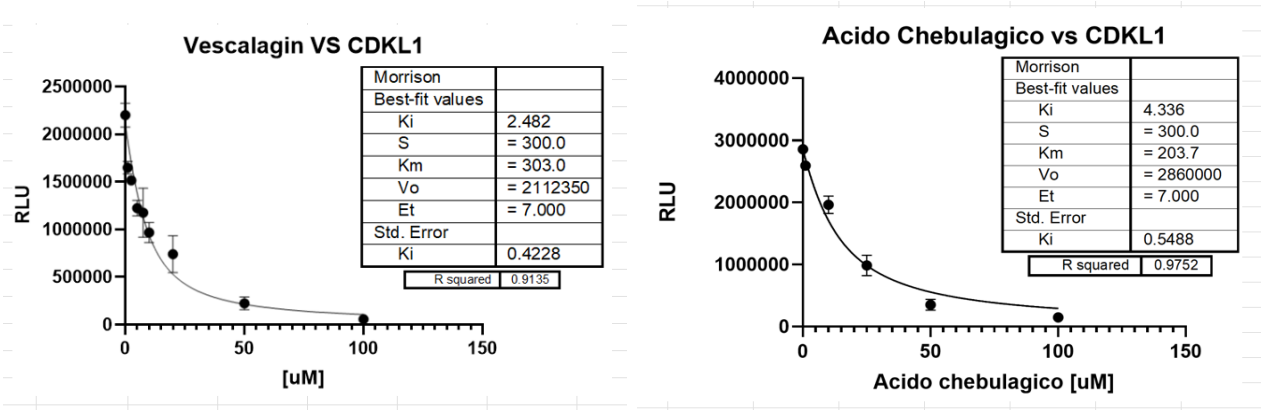

Figure 18. Dose-response curve of CDKL1 inhibition by Vescalagin (left) and Chebulagic Acid (right)

Finally, we had the opportunity to test a small library of compounds synthesized by the group of Prof. Maccioni at the University of Cagliari. These compounds had been developed as potential serine/threonine kinase inhibitors. However, none of the tested molecules showed detectable inhibitory activity toward CDKL1 under the assay conditions employed (Table 7). In the near future, we plan to evaluate additional compounds based on different chemical scaffolds, with the aim of identifying promising hits for the development of more specific CDKL1 inhibitors.

Table 7. Inhibition assays of Cagliari university compounds.

Compound ID	**Inhibition percentage**	
	100 µM	**1 µM**
EMACA 9B	9,39 ± 0,17 %	5,95 ± 2,04 %
EMACA 3G	7,57 ± 0,76 %	7,27 ± 4,14 %
EMACA 6F	8,81 ± 0,01 %	10,40 ± 6,15 %
EMACA 9A	4,98 ± 1,67 %	1,13 ± 0,12 %
EMACA 6D	10,19 ± 0,00 %	0,00%
EMACA 9F	6,50 ± 3,21 %	0,00%
EMACA 6C	7,70 ± 6,46 %	0,00%
EMACA 6A	9,34 ± 9,44 %	10,21 ± 10,01 %
EMACA 3A	4,62 ± 4,26 %	1,27 ± 0,00 %
EMACA 3C	8,65 ± 7,36 %	0,00%
EMACA 9E	9,24 ± 5,13 %	3,32 ± 0,00 %
EMACA 3D	0,00%	0,00%
EMACA 9D	7,10 ± 0,00 %	7,20 ± 4,03 %
EMACA 6B	0,32 ± 0,00 %	0,00%

5. Conclusion and future perspectives

In this thesis, human CDKL1 was expressed, purified, and biochemically characterized with the aim of establishing a reliable in vitro system to study its kinase activity and pharmacological inhibition. CDKL1 remains a poorly characterized member of the CDK-like kinase family, and no standardized biochemical assay for recombinant CDKL1 activity had been previously established. Therefore, an important original contribution of this work was the development of the first in vitro enzymatic platform suitable for measuring CDKL1 kinase activity under controlled experimental conditions.

CDKL1 was successfully expressed in Escherichia coli using a co-expression strategy with λ phosphatase, which was intended to limit potential toxicity associated with the heterologous production of an active eukaryotic kinase in bacterial cells. The recombinant protein was purified through its N-terminal His-tag by immobilized metal affinity chromatography. Initial batch purification allowed enrichment of CDKL1 from the bacterial lysate, and the purification workflow was subsequently improved using an automated chromatographic system. This approach allowed recovery of CDKL1-containing fractions suitable for downstream enzymatic characterization.

A central part of the work was the development of a CDKL1 activity assay. The ADP-Glo™ system was selected as a non-radioactive and sensitive method to quantify kinase activity through measurement of ADP production. Several peptide substrates were tested, and peptide CDKL1-3 (RWGPRPGSSRRGIPP) showed the best performance under the assay conditions employed. This substrate was therefore selected for assay optimization and for subsequent biochemical analyses.

Reaction conditions were optimized by evaluating key parameters including pH, buffer composition, ATP concentration, and substrate concentration. These experiments showed that CDKL1 activity is sensitive to the chemical environment of the reaction and allowed the definition of suitable assay conditions for reproducible activity measurements. Substrate and ATP titrations also provided a first quantitative description of CDKL1 catalytic behavior in vitro, including the apparent affinity for the selected peptide substrate and for ATP.

Once suitable assay conditions had been established, the system was applied to the preliminary evaluation of CDKL1 inhibition by selected compounds. This part of the work included known kinase inhibitors, used as reference compounds, and natural polyphenolic compounds, with particular attention to punicalagin and structurally related ellagitannins. These compounds were of interest because previous kinome-wide screening data suggested that CDKL1 could be among their potential kinase targets. The results obtained in this thesis indicate that CDKL1 activity can be inhibited in vitro by selected ellagitannins, with chebulagic acid and vescalagin emerging as the most active compounds under the assay conditions employed.

The identification of active ellagitannins also opens the possibility of future structural studies. This aspect is particularly relevant because ellagitannins are complex natural products and are not easily accessible by chemical synthesis. This limits the possibility of directly generating large series of analogues through conventional medicinal chemistry approaches. For this reason, one important future objective will be to crystallize CDKL1 in complex with the most active ellagitannins, in particular chebulagic acid and vescalagin. Structural information on these complexes would help define the molecular basis of inhibition and could guide the design or selection of simpler analogues with improved potency, selectivity, and synthetic accessibility.

Another important point for future investigation concerns the activation state of recombinant CDKL1. In many protein kinases, the activation loop is a regulatory region located within the catalytic domain that can influence substrate access, catalytic-site organization, and overall kinase activity. In several kinases, phosphorylation of residues within the activation loop promotes the transition from a less active to a more active conformation. However, the relevance of this mechanism is kinase-dependent and cannot be assumed a priori for CDKL1.

In this thesis, CDKL1 was produced in a bacterial expression system. This approach allowed recombinant protein production and biochemical assay development, but it does not reproduce the full regulatory environment of a eukaryotic cell. Therefore, if CDKL1 activity is modulated by phosphorylation of the activation loop, or by other regulatory phosphorylation events, these modifications may be absent or incomplete in the protein purified from *E. coli*. As a consequence, the activity measured in this work may correspond to a basal or partially activated form of CDKL1 rather than to the fully active enzyme present

in cells.

Future experiments should therefore address whether phosphorylation within the activation loop contributes to CDKL1 regulation. One possible strategy will be to express and purify CDKL1 from eukaryotic cells, such as HEK293 cells, where regulatory phosphorylation events may occur more efficiently. In parallel, non-phosphorylatable and phosphomimetic mutants of candidate residues located in the activation loop could be generated and compared with the wild-type protein. This approach would allow evaluation of whether these residues influence CDKL1 catalytic activity, substrate phosphorylation, or inhibitor sensitivity.

Comparison of CDKL1 purified from bacterial and eukaryotic systems, together with the analysis of activation-loop mutants, will help determine whether the activity measured in vitro depends on phosphorylation events that are not reproduced in bacteria. These experiments will be important to understand whether the assay developed in this thesis already reflects the intrinsic catalytic activity of CDKL1 or whether additional regulatory mechanisms are required to obtain the fully active kinase.

Bibliography

1. Lavoie H, Gagnon J, Therrien M. ERK signalling: a master regulator of cell behaviour, life and fate. Nat Rev Mol Cell Biol. 2020 Oct 23;21(10):607–32. doi:10.1038/s41580-020-0255-7
2. Manning G., Whyte D. B., Martinez R., Hunter T., Sudarsanam S. Manning, G. et al., 2002. Science (1979). 2002 Dec 6;298. doi:DOI:10.1126/science.1075762
3. Ardito F, Giuliani M, Perrone D, Troiano G, Muzio L Lo. The crucial role of protein phosphorylation in cell signalingand its use as targeted therapy (Review). International Journal of Molecular Medicine. Spandidos Publications; 2017. p. 271–80. doi:10.3892/ijmm.2017.3036 PubMed PMID: 28656226.
4. Roskoski R. Properties of FDA-approved small molecule protein kinase inhibitors: A 2024 update. Pharmacological Research. Academic Press; 2024. doi:10.1016/j.phrs.2024.107059 PubMed PMID: 38216005.
5. Smoly I, Shemesh N, Ziv-Ukelson M, Ben-Zvi A, Yeger-Lotem E. An Asymmetrically Balanced Organization of Kinases versus Phosphatases across Eukaryotes Determines Their Distinct Impacts. PLoS Comput Biol. 2017 Jan 30;13(1):e1005221. doi:10.1371/journal.pcbi.1005221
6. Pang K, Wang W, Qin J, Shi Z, Hao L, Ma Y, et al. Role of protein phosphorylation in cell signaling, disease, and the intervention therapy. MedComm (Beijing). 2022 Dec 3;3(4). doi:10.1002/mco2.175
7. of Science A. All You Need to Know About Protein Kinases [Internet]. Available from: https://atlasofscience.org
8. Sakkiah S, Cao GP, Gupta SP, Lee KW. Overview of the Structure and Function of Protein Kinases. Curr Enzym Inhib. 2017 Jun 15;13(2). doi:10.2174/1573408013666161226155608
9. Lemmon MA, Schlessinger J. Cell Signaling by Receptor Tyrosine Kinases. Cell. 2010 Jun;141(7):1117–34. doi:10.1016/j.cell.2010.06.011
10. Lindberg MF, Meijer L. Dual-Specificity, Tyrosine Phosphorylation-Regulated Kinases (DYRKs) and cdc2-Like Kinases (CLKs) in Human Disease, an Overview. Int J Mol Sci. 2021 Jun 3;22(11):6047. doi:10.3390/ijms22116047
11. Chowdhury I, Dashi G, Keskitalo S. CMGC Kinases in Health and Cancer. Cancers (Basel). 2023 Jul 28;15(15):3838. doi:10.3390/cancers15153838
12. Nguyen LK, Matallanas D, Croucher DR, von Kriegsheim A, Kholodenko BN. Signalling by

protein phosphatases and drug development: a systems-centred view. FEBS J. 2013 Jan 14;280(2):751–65. doi:10.1111/j.1742-4658.2012.08522.x

13. Smoly I, Shemesh N, Ziv-Ukelson M, Ben-Zvi A, Yeger-Lotem E. An Asymmetrically Balanced Organization of Kinases versus Phosphatases across Eukaryotes Determines Their Distinct Impacts. PLoS Comput Biol. 2017 Jan 30;13(1):e1005221. doi:10.1371/journal.pcbi.1005221
14. Abbas M, Ali Sami SH, Gajdács M, Tariq MJ. Recent FDA-approved kinase inhibitors for cancer therapy in 2025: A comprehensive review and perspectives. EXCLI J. 2025;24:1609–33. doi:10.17179/excli2025-8972 PubMed PMID: 41584508.
15. Cohen, P., 2002_examples.
16. Amusan OT, Guo H. CMGC Kinases in Viral Infection and Human Disease. Pathogens. Multidisciplinary Digital Publishing Institute (MDPI); 2026. doi:10.3390/pathogens15040366
17. Taylor SS, Kornev AP. Protein kinases: Evolution of dynamic regulatory proteins. Trends in Biochemical Sciences. 2011. p. 65–77. doi:10.1016/j.tibs.2010.09.006 PubMed PMID: 20971646.
18. Li C, Liu Y, Luo S, Yang M, Li L, Sun L. A review of CDKL: An underestimated protein kinase family. International Journal of Biological Macromolecules. Elsevier B.V.; 2024. doi:10.1016/j.ijbiomac.2024.133604 PubMed PMID: 38964683.
19. Malumbres M. Cyclin-dependent kinases. Genome Biol. 2014;15(6). doi:10.1186/gb4184 PubMed PMID: 25180339.
20. Canning P, Park K, Gonçalves J, Li C, Howard CJ, Sharpe TD, et al. CDKL Family Kinases Have Evolved Distinct Structural Features and Ciliary Function. Cell Rep. 2018 Jan 23;22(4):885–94. doi:10.1016/j.celrep.2017.12.083 PubMed PMID: 29420175.
21. Katayama S, Sueyoshi N, Inazu T, Kameshita I. Cyclin-Dependent Kinase-Like 5 (CDKL5): Possible Cellular Signalling Targets and Involvement in CDKL5 Deficiency Disorder. Neural Plasticity. Hindawi Limited; 2020. doi:10.1155/2020/6970190 PubMed PMID: 32587608.
22. Flax RG, Rosston P, Rocha C, Anderson B, Capener JL, Durcan TM, et al. Illumination of understudied ciliary kinases. Frontiers in Molecular Biosciences. Frontiers Media SA; 2024. doi:10.3389/fmolb.2024.1352781
23. Lin M, Zhang Y, Li A, Tang E, Peng J, Tang W, et al. High-throughput RNAi screening of human kinases identifies predictors of clinical outcome in colorectal cancer patients treated with oxaliplatin. Oncotarget [Internet]. 2015. Available from: www.impactjournals.com/oncotarget/
24. Qin C, Ren L, Ji M, Lv S, Wei Y, Zhu D, et al. CDKL1 promotes tumor proliferation and invasion

in colorectal cancer. Onco Targets Ther. 2017 Mar 16;10:1613–24. doi:10.2147/OTT.S133014

25. Yen S, Kenessey A, Lee SC, Dickson DW. The Distribution and Biochemical Properties of a Cdc2-Related Kinase, KKIALRE, in Normal and Alzheimer Brains. J Neurochem. 1995 Dec;65(6):2577–84. doi:10.1046/j.1471-4159.1995.65062577.x PubMed PMID: 7595554.
26. Sun W, Yao L, Jiang B, Shao H, Zhao Y, Wang Q. A role for Cdkl1 in the development of gastric cancer. Acta Oncol (Madr). 2012 Jul;51(6):790–6. doi:10.3109/0284186X.2012.665611 PubMed PMID: 22369697.
27. Hsu LS, Liang CJ, Tseng CY, Yeh CW, Tsai JN. Zebrafish cyclin-dependent protein kinase-like 1 (zcdkl1): Identification and functional characterization. Int J Mol Sci. 2011 Jun;12(6):3606–17. doi:10.3390/ijms12063606 PubMed PMID: 21747697.
28. Li Z, Xue H, Li J, Zheng Z, Liu Z, Dong X, et al. CDKL1 potentiates the antitumor efficacy of radioimmunotherapy by binding to transcription factor YBX1 and blocking PD-L1 expression in lung cancer. Journal of Experimental and Clinical Cancer Research. 2024 Dec 1;43(1). doi:10.1186/s13046-024-03007-w PubMed PMID: 38520004.
29. Tang L, Gao Y, Yan F, Tang J. Evaluation of Cyclin-Dependent Kinase-Like 1 Expression in Breast Cancer Tissues and Its Regulation in Cancer Cell Growth. Cancer Biother Radiopharm. 2012 Aug;27(6):392–8. doi:10.1089/cbr.2012.1198
30. Song Z, Lin J, Sun Z, Ni J, Sha Y. RNAi-mediated downregulation of CDKL1 inhibits growth and colony-formation ability, promotes apoptosis of human melanoma cells. J Dermatol Sci. 2015 Jul 1;79(1):57–63. doi:10.1016/j.jdermsci.2015.03.020 PubMed PMID: 25920913.
31. Li K, Meng Z, Jiang L, Xia C, Xu K, Yuan D, et al. CDKL1 promotes the chemoresistance of human oral squamous cell carcinoma cells to hydroxycamptothecin. Mol Cell Probes. 2019 Apr 1;44:57–62. doi:10.1016/j.mcp.2019.02.004 PubMed PMID: 30802495.
32. Yamada H, Wakamori S, Hirokane T, Ikeuchi K, Matsumoto S. Structural revisions in natural ellagitannins. Molecules. MDPI AG; 2018. doi:10.3390/molecules23081901 PubMed PMID: 30061530.
33. Landete JM. Ellagitannins, ellagic acid and their derived metabolites: A review about source, metabolism, functions and health. Food Research International. 2011. p. 1150–60. doi:10.1016/j.foodres.2011.04.027
34. Turrini E, Ferruzzi L, Fimognari C. Potential effects of pomegranate polyphenols in cancer prevention and therapy. Oxidative Medicine and Cellular Longevity. Hindawi Publishing

Corporation; 2015. doi:10.1155/2015/938475 PubMed PMID: 26180600.

35. Čižmáriková M, Michalková R, Mirossay L, Mojžišová G, Zigová M, Bardelčíková A, et al. Ellagic Acid and Cancer Hallmarks: Insights from Experimental Evidence. Biomolecules. Multidisciplinary Digital Publishing Institute (MDPI); 2023. doi:10.3390/biom13111653
36. Lu G, Wang X, Cheng M, Wang S, Ma K. The multifaceted mechanisms of ellagic acid in the treatment of tumors: State-of-the-art. Biomedicine and Pharmacotherapy. Elsevier Masson s.r.l.; 2023. doi:10.1016/j.biopha.2023.115132 PubMed PMID: 37423169.
37. Ceci C, Lacal PM, Tentori L, De Martino MG, Miano R, Graziani G. Experimental Evidence of the Antitumor, Antimetastatic and Antiangiogenic Activity of Ellagic Acid. Nutrients. 2018 Nov 14;10(11):1756. doi:10.3390/nu10111756
38. Wang Neng. ELLAGIC ACID EXERTS ANTI-ANGIOGENESIS EFFECTS BY BLOCKING VEGFR-2 SIGNALING PATHWAY IN BREAST CANCER WANG NENG. [Hong Kong]: University of Hong Kong; 2012.
39. Meng X, Cui Z, Shi H, Ma X, Li W, Liu X, et al. Ellagic acid inhibits cell proliferation, migration, and invasion of anaplastic thyroid cancer cells via the Wnt/β-catenin and PI3K/ Akt pathways. Acta Biochim Pol. 2023;70(1):109–15. doi:10.18388/abp.2020_6317 PubMed PMID: 36773307.
40. Yousuf M, Shamsi A, Khan P, Shahbaaz M, Alajmi MF, Hussain A, et al. Ellagic acid controls cell proliferation and induces apoptosis in breast cancer cells via inhibition of cyclin-dependent kinase 6. Int J Mol Sci. 2020 May 2;21(10). doi:10.3390/ijms21103526 PubMed PMID: 32429317.
41. Dongliang W, Chen Q, Tan Y, Liu B, Liu C. Ellagic acid inhibits human glioblastoma growth in vitro and in vivo. Oncol Rep. 2017 Feb 1;37(2):1084–92. doi:10.3892/or.2016.5331 PubMed PMID: 28035411.
42. Johnson JL, Yaron TM, Huntsman EM, Kerelsky A, Song J, Regev A, et al. An atlas of substrate specificities for the human serine/threonine kinome. Nature. 2023 Jan 26;613(7945):759–66. doi:10.1038/s41586-022-05575-3
43. Prade L, Engh RA, Girod A, Kinzel V, Huber R, Bossemeyer D. Staurosporine-induced conformational changes of cAMP-dependent protein kinase catalytic subunit explain inhibitory potential. Structure. 1997 Dec;5(12):1627–37. doi:10.1016/S0969-2126(97)00310-9
44. Iyer GH, Taslimi P, Pazhanisamy S. Staurosporine-based binding assay for testing the affinity of compounds to protein kinases. Anal Biochem. 2008 Feb;373(2):197–206. doi:10.1016/j.ab.2007.11.004